Development and Maintenance of Force and Stiffness in Airway Smooth Muscle

by

Brandon Anthony Norris

B.Sc., McGill University, 2012

A THESIS SUBMITTED IN PARTIAL FULFILLMENT OF THE REQUIREMENTS FOR

THE DEGREE OF

MASTER OF SCIENCE

in

THE FACULTY OF GRADUATE AND POSTDOCTORAL STUDIES

(Experimental Medicine)

THE UNIVERSITY OF BRITISH COLUMBIA

(Vancouver)

September 2015

ABSTRACT

The primary function of airway smooth muscle (ASM) is to contract upon stimulation. Mechanical manifestation of contraction includes development and maintenance of force and stiffness, and when the developed force is greater than the load on the muscle, shortening occurs. Dysfunction of ASM could lead to excessively stiff or narrowed airways. This thesis research is aimed at advancing our understanding of the basic mechanisms involved in the development and maintenance of force and stiffness in ASM and how these mechanical properties are regulated by enzymes and their associated signalling pathways. The research is also aimed at identifying new targets for asthma therapy with specific interventions that reduce airway stiffness and narrowing. Recently, stiffness of the passive components of ASM –unrelated to that stemming from attached myosin crossbridges - has been shown to be actively regulated by intracellular enzymes. Chapter 2 of this thesis shows that the passive components of the ASM can be activated to generate force and augment stiffness. This activation is cross-bridge independent, as the calcium within the ASM cells was removed and the phosphorylation of the regulatory myosin light chain was abolished. The activation could be prevented when Rho-kinase was inhibited. Rho-kinase is known to be actively involved in the cytoskeletal dynamics of ASM; therefore, it is reasonable to assume that the cytoskeletal network is at least partly responsible for the activation of the passive components in ASM.

Chapter 3 of the thesis aimed to explain the biphasic response that occurs when a ramp stretch is applied to an activated ASM strip. By performing ramp stretches in different conditions, the two phases of the biphasic force response revealed an intricate relationship between the two contributors to muscle stiffness – the attached actomyosin crossbridges and the cytoskeleton.

Results presented in both chapters of the thesis suggest that signalling pathways involving Rho-kinase is crucial for regulating the calcium dependent and independent ASM force and stiffness. This has provided a focus for future studies in identifying enzyme or structural protein targets for modulating ASM mechanical properties down stream of the Rho-kinase.

PREFACE

This thesis is based on experiments done in Dr. Chun Seow's and Dr. Peter Pare's laboratory in the Center for Heart and Lung Innovation at St. Paul's Hospital.

Chapter 1 is based on a published review: B Lan*, BA Norris*, JC Liu, PD Pare, CY Seow, L Deng (* Co-First author). 2014. Development and Maintenance of Force and Stiffness in Airway Smooth Muscle. *Canadian Journal of Physiology and Pharmacology*. Vol. 93, pp. 163-169. The review was written in collaboration with lab members, where certain sections were written by me.

Chapter 2 is based on data collected primarily by me. Biomechanics and ©Kinexus protein shipment were done by me. MLC20 phosphoylation data collection was performed by Dr. Lu Wang. Protein phosphorylation quantification was performed by Kinexus. Experiment protocol was developed by Dr. Seow, Dr. Pare, and me. All data analysis and writing was done by me and Dr. Seow. Figures were done by me, with the exception of figure 2.4 (Dr. Lu Wang).

Chapter 3 is based on published research: Brandon A. Norris, Bo Lan, Lu Wang, Christopher D. Pascoe, Nicholas E. Swyngedouw, Peter D. Paré, and Chun Y. Seow. 2015. Biphasic force response to iso-velocity stretch in airway smooth muscle. *American Journal of Physiology – Lung Cellular and Molecular Physiology*. The experiments were designed by Dr. Seow, Dr. Pare, Bo Lan, and me. All experiments were performed by me, with the one exception of the data in figure 3.4 which was obtained by Bo Lan. The published manuscript was written by Dr. Seow and myself.

The work in this thesis is covered under the Human Ethics Board of UBC certificate number H12-02487, project title "Plasticity in airway smooth muscle".

TABLE OF CONTENTS

LIST OF TABLES

LIST OF FIGURES

LIST OF ABBREVIATIONS

A23187   – Calcium ionophore drug

AC   – Alternating current

ACh   – Acetylcholine

ANOVA   – Analysis of variance

ASM   – Airway smooth muscle

ATP   – Adenosine triphosphate

BSA   – Bovine serum albumin

Ca^{2+} – Calcium ions

$[Ca^{2+}]_i$ – Cytosolic calcium

$CaCl_2$ – Calcium chloride

CO_2 – Carbon dioxide

CPA   – Cyclopiazonic acid

CPI-17   – C-kinase potentiated protein phosphatase-1 inhibitor

CPM   – Counts per minute

DI   – Deep inspiration

DTT   – Dithiothreitol

EFS   – Electrical field stimulation

EDTA   – Ethylenediaminetetraacetic acid

EGTA   – Ethylene glycol tetraacetic acid

ECM   – Extracellular matrix

F_{max} – Maximal isometric force

F-actin   – Filamentous actin

G-actin	–	Globular actin
GF109203x	–	PKC inhibitor
GPCR	–	G-protein coupled receptor
H1152	–	Rho-kinase inhibitor
Hz	–	Hertz
IP_3	–	Inositol 1,4,5-trisphosphate
K^+	–	Potassium
KCl	–	Potassium Chloride
L_{ref}	–	Reference Length
M3	–	Muscarinic 3 receptor
ML-7	–	MLCK inhibitor
MLC20	–	Myosin light chain
MLCK	–	Myosin Light Chain Kinase
MLCP	–	Myosin Light chain phosphatase
min	–	Minute
mm	–	Millimeter
mM	–	Millimolar
mN	–	Millinewton
ms	–	Millisecond
MYPT1	–	Myosin phosphatase-targeting subunit 1
$NaCl_2$	–	Sodium chloride
$NaHCO_3$	–	Sodium bicarbonate
NaH_2PO_4	–	Sodium phosphate monobasic
O_2	–	Oxygen

PKC   – Protein Kinase C

s   – Second(s)
SE   – Standard error
SERCA   – Sarco/endoplasmic reticulum Ca2+-ATPase.
SM   – Smooth muscle
S_{max} – Max stiffness
SMC   – Smooth muscle cell(s)
SR   – Sarcoplasmic Reticulum

TBS   – Tris-base saline
TBST   – Tris-base saline with tween
TCA   – Trichloroacetic acid

μM   – Micromolar

ACKNOWLEDGEMENTS

I have many people to acknowledge and thank for the success of this degree. First, I want to thank both of my supervisors: Without you, it may have taken me quite some time to find my stride after my McGill degree. I have spent the last 2 years of this degree, and 1 year prior to that, learning the skill sets you have, which have obviously taken decades to nurture. Dr. Seow, I have always had a very high interest in mathematics and physics, and I am so lucky to have joined a lab where you have the expertise in implementing these skills to biology. It has been a tough road to learn some of these skills, but I have come out a much better scientist. Dr. Pare, to this day you baffle me with your ability to ask questions nobody would ever think of. Your understanding of the scientific method is so vast that, irrespective of the health science being presented, you can constructively criticize it and offer sound advice. I aspire to someday have this wisdom.

I would like to thank members of the Seow lab, including Dr. Zhang, Dr. Wang, and Mr. Solomon. Also, the students of the lab, Dr. Bo Lan, Dr. Chris Pascoe, Jeff Lui, and Nick Swyngedouw. Bo, you have been a great mentor to me, and our overlapping interest in biomechanics has flourished a great friendship. Chris, you have been an unbelievable role model, your knowledge and skillset is far beyond their years. Jeff, you have always kept things light, and have been a great friend. Nick, without you this last year would have been much more challenging. Things have been a lot of fun and I cherish our friendship.

DEDICATION

I would like to dedicate this thesis to my four grandparents: Jack, Joyce, Antonio, and Rosa.

Chapter 1   Introduction[1]

1.1   General introduction

Without question, our current understanding of the contractile mechanism in smooth muscle is far behind both that of skeletal and cardiac muscle. This elusive tissue lines the wall of many hollow organs within the body, some of which are the airways, stomach, blood vessels, intestines, and bladder. Structural integrity is one of the known roles of smooth muscle, as it controls the shape, size, and mechanical properties such as distensibility of these organs. Therefore, malfunction of the muscle can manifest as diseases associated with each of these organs.

One example of this is asthma, a disease of the airway where patients have recurring episodes of impaired breathing, typically caused by airway constriction and airway inflammation. The airway smooth muscle (ASM) is ultimately responsible for the narrowing of the airway, and for this reason, ASM has been a focus of study in asthma (Doeing and Solway 2013). A current method to treat asthma consists of inhaling bronchodilators (β2 agonists); the agonists work by relaxing the ASM and thus making the airways less narrow and more distensible (Cazzola et al. 2012). However, this treatment is not perfect; in more severe cases of asthma, bronchodilators are less effective (Gamble et al. 2009). Therefore, development of drugs aiming at new targets within ASM will improve treatment of the disease.

To this point, elucidation of the contractile mechanism in ASM is important for the treatment of the disease. ASM contraction can be divided into two phases: the initial phase associated with active force development and the sustained phase associated with maintenance of the developed force. The initial phase is largely controlled by the activation of actomyosin interaction through phosphorylation of the myosin light chain (MLC20) (Frearson, Focant, and Perry 1976; A. Sobieszek 1977), whereas the mechanism responsible for force maintenance in the sustained phase is less clear.

---

[1] Parts of the chapter have been published. Bo Lan*, Brandon A. Norris*, Jeffrey C.-Y. Liu, Peter D. Pare, Chun Y. Seow, and Linhong Deng. Development and maintenance of force and stiffness in airway smooth muscle. CJJP 2014. (*, co-first authors)

In ASM, evidence of an interesting phenomenon has accumulated in the last few years: muscle stiffness can be uncoupled from active force, suggesting that subcellular structures other than actomyosin cross-bridges are capable of maintaining force and stiffness (Bosse et al. 2010; Raqeeb et al. 2012; Lan et al. 2013). In vascular smooth muscle, it has been shown that agonist stimulation results in better maintenance of force compared with stimulation by high $[K^+]$ induced membrane depolarization (Morgan and Morgan 1984). This suggests that agonist stimulation through G-protein coupled receptor (GPCR) may activate signalling pathways other than the one that activates actomyosin interaction. One of the pathways that agonists of GPCR may activate regulates the cytoskeleton of ASM; regulation of the cytoskeleton is currently a hot area of research in the ASM field (Zhang and Gunst 2008).

The cytoskeleton is a potential new target for modulating ASM contractility distinct from the actomyosin cross-bridge cycle, as studies have shown that impairing the remodelling process of this dynamic filament network leads to a decrease in contractility of the ASM (Tseng et al. 1997; Youn, Kim, and Hai 1998; Mehta and Gunst 1999; Dowell et al. 2005; Tang, Turner, and Gunst 2003; Opazo Saez et al. 2004; Huang, Zhang, and Gunst 2011; Huang, Day, and Gunst 2014). It has been shown that ASM force could be reduced by interrupting cytoskeletal dynamics without a change in MLC20 phosphorylation [Tang 2003, Zhang 2005]; this suggests that at least some of the pathways regulating the dynamics of the cytoskeleton are independent from those regulating the cross-bridge cycle. This means pathways outside of the cross-bridge cycle, but within the cytoskeleton, can control force production of the ASM, thus pointing to possibilities for finding new targets in the treatment of asthma.

In this introduction, a focus on the pathways regulating ASM force and stiffness will be reviewed –specifically their development and maintenance. Literature on the cytoskeletal network will be discussed, as this area of research is currently quite active within the ASM field.

1.2   Development of force and stiffness in ASM

1.2.1   Force development regulated via MLC20 phosphorylation

The fundamental molecular mechanism for contraction in both smooth and striated muscles is essentially the same; development of active force or generation of shortening is due to cyclical interaction of myosin cross-bridges with actin filaments (Huxley 1957). In smooth muscle, actomyosin interaction is activated by calcium dependent phosphorylation of MLC20 (Frearson, Focant, and Perry 1976; A. Sobieszek 1977). The phosphorylation is initiated by an increase in the cytosolic concentration of Ca^{2+} ($[Ca^{2+}]_i$). Influx of calcium into the cytosol occurs via the voltage-dependent and/or receptor-activated calcium channels on the sarcolemma. The sarcoplasmic reticulum (SR) also releases calcium into the cytosol through the inositol 1,4,5-trisphosphate (IP_3) gated calcium channels or through the ryanodine receptors. Calcium in the cytosol binds to calmodulin to form the Ca^{2+}-calmodulin complex, which binds to the myosin light chain kinase (MLCK) thus activating the kinase and allowing it to phosphorylate MLC20. There is a parallel antagonistic pathway to MLCK, and that is, the MLC20 phosphatase (MLCP) pathway. MLCP counteracts the action of MLCK by dephosphorylating MLC20. Pathways activated by GPCR agonists in smooth muscle are known to inhibit MLCP. These pathways include Rho-kinase and protein kinase C (PKC) pathways (Somlyo and Somlyo 2004; Puetz, Lubomirov, and Pfitzer 2009). The extent of MLC20 phosphorylation in activated smooth muscle is thus determined by the relative activities of MLCK and MLCP. Inhibition of MLCP will lead to an increase in MLC20 phosphorylation even when $[Ca^{2+}]_i$ remains the same. This phenomenon is referred to as calcium sensitization. The specific mechanism is as follows. When Rho-kinase is activated it phosphorylates the myosin phosphatase-targeting subunit 1 (MYPT1) resulting in reduced MLCP activity. PKC and Rho-kinase can also phosphorylate a phosphoprotein CPI-17. Phosphorylated CPI-17 binds to the catalytic subunit of MLCP and inhibits the phosphatase activity. The inhibition of MLCP via both Rho-kinase-catalyzed phosphorylation of MYPT1 and phosphorylated CPI-17 can induce an increase in MLC20 phosphorylation without a change in cytosolic calcium. Calcium sensitization plays an important role in both the initial and sustained phases of contraction in smooth muscle.

1.2.2   Cytoskeleton and force development

Although actomyosin interaction is the dominant process that generates force in ASM, the cytoskeleton also undergoes dynamic changes which are critical for the development of maximal force. The mechanism by which the cytoskeletal elements interact with one another has yet to be fully elucidated, but recent research has unveiled some important roles for the cytoskeleton in force transmission during force development.

The role of actin in force development

Actin is the most abundant protein in smooth muscle cells, and only a minor fraction of the actin filaments inside the cell are in direct contact with the myosin filaments (Herrera, Martinez, and Seow 2004). This begs the question, what is the purpose of actin filaments besides their participation in actomyosin interaction? It is well established that polymerization of cytoskeletal actin is necessary for maximal ASM contraction, as inhibition of this process causes sub-maximal contraction (Tseng et al. 1997; Youn, Kim, and Hai 1998; Mehta and Gunst 1999; Dowell et al. 2005). It is interesting to note that although the polymerization of actin allows for maximal contraction, the percent change of G-actin (globular) to F-actin (filamentous) is quite small (Hirshman et al. 1998; Jones et al. 1999). Furthermore, inhibition of actin polymerization has no effect on MLC20 phosphorylation (Tang, Turner, and Gunst 2003; Zhang et al. 2005). This suggests that the reduction in the developed force due to inhibition of actin polymerization is not because the myosin cross-bridges are not fully activated, but rather that the transmission of developed force to the extracellular domain is impaired. Force development and force transmission are therefore likely regulated by separate signal pathways, with the former related to actomyosin interaction and the latter related to cytoskeleton stabilization.

Protein assembly near the cell membrane facilitating force transmission

The mechanism that enables smooth muscle to transmit force generated by the cross-bridges to the extracellular domain involves many cytoskeletal proteins (Zhang and Gunst 2008). To transmit force, actin filaments must be attached to the adhesion plaques inside the cells; the

adhesion plaques also connect to the extracellular matrix (ECM) or adjacent smooth muscle cells. These actin filaments include those closely associated with myosin filaments that partake in the actomyosin interaction, but also likely include those not directly associated with myosin; instead, they are connected to other actin filaments or dense bodies within the cell to form a filament network (cytoskeleton). There are an array of proteins that anchor actin filaments to the ECM via integrins (Zhang and Gunst 2008; Opazo Saez et al. 2004; Kim, Hoque, and Hai 2004; Zhang and Gunst 2006). At the onset of contraction there is movement of these cytoskeletal adapter proteins towards the membrane. An example of this is α-actinin, which is an actin binding protein that has also been shown to bind to β-integrin (Zhang and Gunst 2006). It has been shown that cytosolic α-actinin is recruited to the membrane when ASM is activated by carbachol (Kim, Hoque, and Hai 2004). In a similar study by Zhang and Gunst, α-actinin is recruited to the vicinity of the integrin when ASM is activated by acetylcholine (Zhang and Gunst 2006). They also evaluated the role of α-actinin in force transmission and found that by inhibiting the migration of this protein to the cell membrane, force was markedly reduced whereas MLC20 phosphorylation was unchanged, demonstrating a clear distinction between the regulation of actomyosin interaction and cytoskeletal dynamics.

Along with α-actinin, other proteins such as vinculin and paxillin are involved with anchorage of actin filaments to focal adhesion sites. Paxillin is phosphorylated during contractile stimulation (Z. Wang, Pavalko, and Gunst 1996), and it is known that with a non-phosphorylatable paxillin in ASM, actin is unable to polymerize during activation (Tang, Turner, and Gunst 2003). Vinculin is also to be recruited to the cell membrane where it binds to actin, and disruption of the recruitment results in decreased contraction (Huang, Zhang, and Gunst 2011; Opazo Saez et al. 2004; Huang, Day, and Gunst 2014). With the evidence presented here, a convincing argument can be made that both activation of the actomyosin interaction and the recruitment of cytoskeletal proteins to the cell membrane are necessary for force development in ASM. A logical explanation for these observations is that the contractile filaments need to be mechanically coupled to adjacent cells and/or the ECM in order for the intracellularly developed force to be transmitted to the extracellular world.

1.2.3   Stiffness development during cross-bridge activation

Both active force development and tensile stiffness are associated with the actomyosin interaction. Stiffness measured during activation of ASM is dramatically higher compared to that in the relaxed state, due to the cross-bridging between the myosin and actin filaments. There is a wealth of data suggesting that the increase in stiffness is in parallel with the increase in MLC20 phosphorylation; a linear relationship between stiffness and MLC phosphorylation has been reported (Kamm and Stull 1986). However, the relationship between stiffness and active force is curvilinear (S. J. Gunst et al. 1995); stiffness and phosphorylation of MLC20 increase more rapidly than isometric force during activation (Word, Tang, and Kamm 1994; Kamm and Stull 1986; Tanner, Haeberle, and Meiss 1988). One explanation for this phenomenon is that in the initial state of attachment, a cross-bridge is in a low-force state and does not contribute to force development. However, any attached cross-bridges contribute to stiffness even if they are in the low-force state. Force development occurs after the initial state during the transition from the low-force state to the high-force state in a process called the power-stroke. It is believed that during activation, each cross-bridge goes through the ATP-dependent attachment-detachment cycle independently. This allows each bridge to work as an independent generator of force. This also explains why changes in muscle stiffness precede that of force during force development; the whole population of attached cross-bridges contribute to muscle stiffness, but only those undergoing the power-strokes contribute to force development.

1.2.4   Stiffness of the activated ASM cytoskeleton

Measuring the stiffness of the cytoskeleton during contraction is difficult. This is because during contraction the overwhelming contribution to muscle stiffness is from actomyosin cross-bridge interaction. Separating the stiffness stemming from the cross-bridges and the cytoskeleton is a challenge because many of the pathways that activate the cross-bridges are in common with those that activate the cytoskeleton (Amano, Nakayama, and Kaibuchi 2010; Puetz, Lubomirov, and Pfitzer 2009; Zhang, Huang, and Gunst 2012). In an effort to study the stiffness of the cytoskeleton, Lan et al used a skinned tracheal smooth muscle preparation that was able to respond (in terms of changes in stiffness) to calcium or acetylcholine (ACh) stimulation,

separately or in combination, without a change in force (Lan et al. 2013). The study revealed that cytoskeletal stiffness - defined by the stiffness not associated with active force development - can be increased when calcium or ACh is added to the bathing solution of the skinned preparation. Interestingly, ACh without calcium was able to induce an increase in stiffness, as was calcium without ACh, without increasing the resting tension. When added together (calcium and ACh), the stiffness increase was equal to the sum of the individual increases of stiffness induced by each stimulant separately. This suggests that they induce stiffness via different pathways. The authors speculated that ACh activation, mediated via G-protein coupled receptors, led to stabilization or solidification of the cytoskeleton (Lan et al. 2013).

The calcium-dependent passive stiffness in resting smooth muscle has often been thought to be associated with the actomyosin interaction that persists in the relaxed state (Siegman et al. 1976). Raqueeb et al examined the redevelopment of passive stiffness after strain softening – a procedure where muscle tissue is subjected to oscillatory strain to break any linkages (responsible for stiffness) inside the cell. The study showed that the redevelopment of stiffness has both a calcium dependent and calcium independent component. Most striking is that after strain softening passive stiffness is able to recover to pre-strain softened values even when active force is inhibited. This suggests that the development of passive stiffness is not dependent on active actomyosin interaction, and implicates the cytoskeleton as a player in the development of stiffness.

1.2.5   The Rho-kinase pathway and its facilitation of cytoskeletal activation

As discussed above, the Rho-kinase pathway is known to be involved in calcium sensitization but more recent research has revealed that Rho-kinase is also involved in the regulation of cytoskeletal dynamics in smooth muscle. Hirshman et al showed that actin reorganization in stimulated ASM cells can be blocked by inhibition of Rho (Hirshman et al. 1998). A later study shows that actin re-organization mediated by RhoA (upstream of Rho-kinase) is an active player in ASM tension development (Zhang, Du, and Gunst 2010). When RhoA is inhibited, the muscle is unable to generate maximal force. Even when the Rho-kinase mediated inhibition of MLCP is blocked, no significant increase in contraction is observed. This

suggests that attenuation of force by inhibition of RhoA likely acts through interference with cytoskeletal organization rather than by affecting actomyosin interaction through MLCP. It has also been shown that actin polymerization and proteins (such as paxillin and vinculin) assembly at the integrin adhesion sites are regulated by RhoA through Rho-kinase mediated phosphorylation (Zhang, Huang, and Gunst 2012).

Passive stiffness has been shown to be sensitive to Rho-kinase inhibition (Raqeeb et al. 2012; Lan et al. 2013; Lan et al. 2015). In skinned ASM strips, the increase in stiffness due to ACh activation in the absence of calcium could be completely reversed by a Rho-kinase inhibitor (H1152) (Lan et al. 2013). Also in ASM strips the redevelopment of calcium-independent passive stiffness after strain softening was attenuated by a Rho-kinase inhibitor (Raqeeb et al. 2012). It can be concluded from these studies that at least part of the passive stiffness is intracellular in origin because Rho-kinase only resides in the intracellular domain. Also, the intracellular calcium-independent stiffness likely has its origin in the cytoskeleton, because changes in the stiffness can be totally uncoupled from active force development.

1.3 Maintenance of force and stiffness in ASM

1.3.1 Latch-bridge model and force maintenance

The ability of smooth muscle to maintain force during a sustained contraction at low energy cost has traditionally been attributed to the development of latch-bridges, which are myosin cross-bridges that are dephosphorylated but remain attached to actin filaments (Hai and Murphy 1988). The latch-bridge state is described as a state in which smooth muscle force can be maintained with low ATP utilization. It is believed that the latch state happens after the early phase of active force development. The findings that led to the latch bridge hypothesis are: a long duty cycle of myosin head associated with low MLC20 phosphorylation and a slow cycling rate of myosin detachment and re-attachment. This explains the slow rate of shortening velocity in the sustained phase of smooth muscle contraction (Dillon et al. 1981). There are, however, lines of evidence that are not consistent with the latch bridge hypothesis. For example, lack of

correlation between shortening velocity and MLC20 phosphorylation have been observed (Merkel, Gerthoffer, and Torphy 1990; Miller-Hance and Kamm 1991).

Alternatives to the latch bridge hypothesis that explain the decreased shortening velocity of smooth muscle over time have been proposed. The alternative mechanisms include caldesmon binding to myosin as a source of "latch bridge" (Roman et al. 2014; Apolinary Sobieszek et al. 2010; Walsh and Sutherland 1989) and a series-to-parallel transition of cross-bridge arrangement during contraction (C. Y. Seow, Pratusevich, and Ford 2000). Recent emerging evidence suggests that stiffening of the cytoskeleton (solidification) could play an important role in force maintenance (Trepat et al. 2007; Deng et al. 2006; Bursac et al. 2005; Lan et al. 2013).

1.3.2   Force adaptation: the interaction between actomyosin and cytoskeletal components

Although tension and stiffness are largely cross-bridge dependent, stabilization by "passive" components of the cytoskeleton is thought to be important in the process of force maintenance. The contribution of the cross-bridge independent (passive) components in the sustained phase of contraction has been called force adaptation. The concept of force-adaptation was introduced in papers by Bossé et al. (Bossé et al. 2009; Bossé et al. 2010), where they described an augmented ability of ASM to generate maximal force after the development of muscle tone induced by a sub-maximal dose of ACh. What this means is that when muscle tone is present, the muscle 'adapts' and over time it is able to produce more force in addition to the tone, compared to the maximal force generated by the muscle in the absence of the tone. The authors speculate that the ability of the muscle to increase force production after adaptation to the tone is due to the transfer of load borne by the cross-bridges to passive structures such as the cytoskeleton. This is a plausible explanation for the results observed in the experiment, as shifting ACh induced tone from the cross-bridges to the cytoskeleton would free up cross-bridges and therefore allow the muscle to generate more total force when it is maximally activated.

The transfer of force from the cross-bridges to the cytoskeleton can potentially explain the results of a study by Gunst et al, where they examined stiffness during an isometric

contraction in ASM (S. J. Gunst et al. 1995). The experiment revealed that as force was maintained during contraction, stiffness increased overtime. This suggests that the structure within the ASM cells changes as the contraction progresses from the initial phase to the sustained phase with contractile filaments increasingly anchored to the cytoskeleton and the cytoskeleton progressively stabilized. Fredberg and colleagues have shown that the cytoskeleton is a relatively fragile structure that fluidizes when subject to a large strain (Krishnan et al. 2009). Furthermore actin filament disassembly is at least one factor responsible for the fluidization (Chen et al. 2010). Intriguingly the rapid process of fluidization appears to be triggered by direct mechanical perturbation without the involvement of chemical signalling, in contrast to the relatively slow process of re-solidification that involves actin re-assembly and presumably signalling and biochemical events associated with re-assembly of proteins (Chen et al. 2010).

1.3.3 The role of cytoskeleton in the energy efficient tonic contraction

The energetic cost to maintain developed force in ASM increases when F-actin depolymerization is inhibited (Jones et al. 1999). Although the exact mechanism is not entirely clear, it appears that active rearrangements of the cytoskeleton that involves actin depolymerization (and presumably re-polymerization) are required for efficient transmission of force. An interesting observation made by Jones et al is that phalloidin seems to inhibit the maintenance of force, but has no effect on the peak force obtained during force development. When cytochalasin-D or latruculin-A are used to inhibit actin polymerization, both force development and maintenance are affected (decreased) (Mehta and Gunst 1999). Taken together these results suggest that actin polymerization is necessary for force development, whereas both actin polymerization and depolymerization are necessary for force maintenance.

Proteins involved in actin polymerization and depolymerization likely play important roles in force maintenance in smooth muscle. Cofilin is one candidate protein for a regulatory role in actin polymerization in ASM (Zhao et al. 2008). Cofilin, which is regulated by the RhoA-LimK pathway, is an actin excising protein, and when it is phosphorylated it is no longer able to perform this function. The study by Zhao et al found that when contraction starts, cofilin is dephosphorylated (activated) and therefore able to contribute to actin polymerization. When

cofilin is prevented from becoming activated, actin polymerization is inhibited. It is reasonable to believe that a dynamic pool of G-actin may be important for many cellular processes, and that cofilin may govern the process of actin dynamics involving polymerization and depolymerization during both the activation and maintenance of contraction.

In a more recent study it was found that the protein cortactin has an important role in ASM contraction (R. Wang et al. 2014). Upon contractile activation, cortactin is phosphorylated and binds to profilin-1, another actin stabilizing protein. The study determined that cortactin is an important protein in the regulation of ASM contraction, as it allows for the polymerization of actin. The study also showed that the increase in cortactin phosphorylation continues into the maintenance phase of contraction, suggesting that it may be especially important in governing the maintenance phase of ASM contraction.
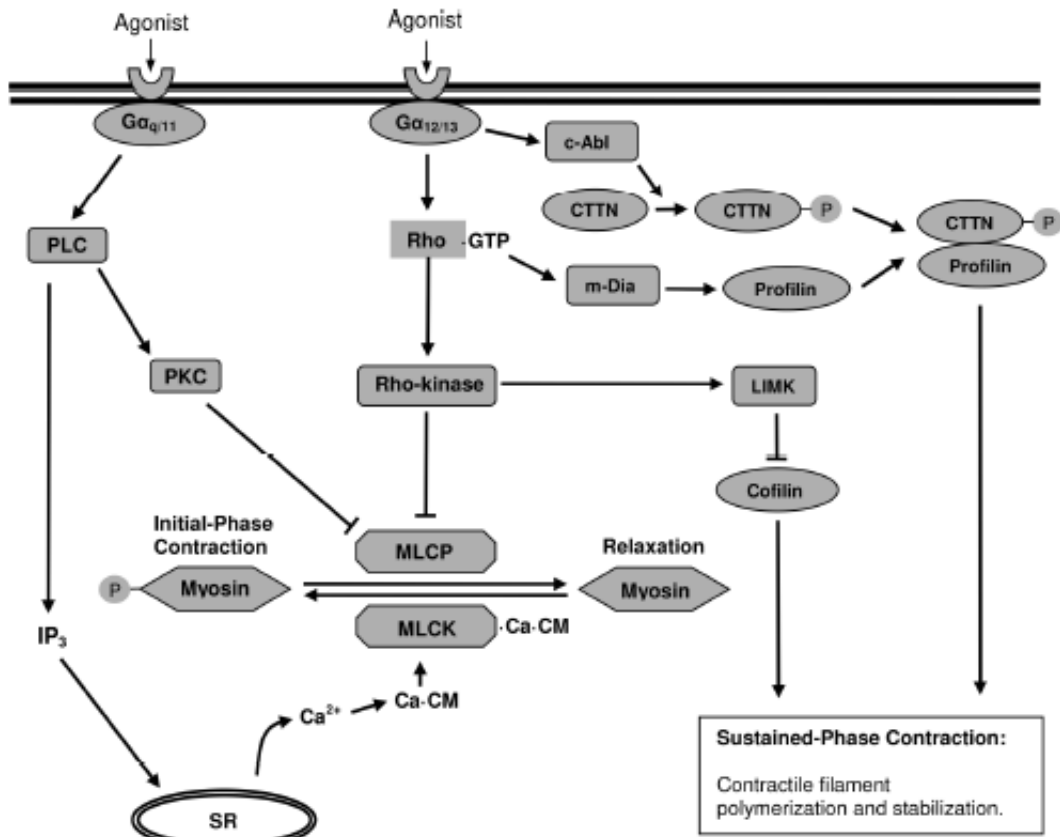
Figure 1.1 Overview of selected pathways of smooth muscle activation. Agonist stimulation of GPCRs leads to simultaneous activation of MLCK and inhibition of MLCP through Rho-kinase and PKC activation. Activation of Rho-kinase also leads to activation of LIMK and polymerization and stabilization of actin filaments through inhibition of cofilin during the sustained phase of contraction. Another pathway leading to actin polymerization and filament stabilization is associated with activation of c-Abl and m-Dia by agonist stimulation that leads to phosphorylation of CTTN by c-Abl and activation of profiling by m-Dia; the activated profilin and phosphorylated cortactin form a complex that induces actin polymerization and filament stabilization. Myosin-P represents myosin with phosphorylated RLC. $G\alpha_{12/13}$, $G\alpha_q$, $G\alpha_s$, heterotrimeric G-proteins with different α subunits associated with GPCR; Rho·GTP, small G proteins (also called RhoA); GPCRs, G-protein coupled receptors; MLCK, myosin light chain kinase; MLCP, myosin light chain phosphatase; PLC, phospholipase C; PKC, protein kinase C; LIMK, LIM kinase; CM, calmodulin; SR, sarcoplasmic reticulum; CTTN, cortactin; RLC, regulatory light chain. (Lan et al. 2014, permission to use figure granted from CJPP – August 2015).

1.4   ASM force development and maintenance in the dynamic environment of the lung in health and asthma

Deep inspirations (DI) are known to reverse experimentally induced broncho-constriction in non-asthmatic human subjects, and interestingly the bronchodilatory effect of DI is largely absent in asthmatic subjects (Skloot, Permutt, and Togias 1995; Kapsali et al. 2000). Furthermore it has been shown that the bronchoprotective effect (i.e., DIs taken before bronchial challenge) is stronger than the bronchodilatory effect (i.e., DIs taken after bronchochallenge) (Kapsali et al. 2000) and that the absence of the bronchoprotective effect of DI is associated with the airway hyperresponsiveness seen in asthma (Scichilone et al. 2001). Avoidance of DI has also been shown to cause airway hyperresponsiveness in non-asthmatic subjects (Chapman et al. 2010). Whether the DI effect is mediated through ASM is still under debate (Noble 2013; Harvey, Parameswaran, and Lutchen 2013; Noble et al. 2014). In isolated relaxed ASM strips it has been shown that oscillatory strain with amplitude comparable to that in vivo induced by DI causes a significant decrease in active force in the subsequent contraction (L. Wang, Pare, and Seow 2000). It has been shown recently in ASM strips that a prior DI-like stretch makes the muscle more compliant, implying that a prior DI may make the subsequent DI more effective in maintaining airway patency (Pascoe et al. 2014). A study (Chin et al. 2012) examining the response to oscillatory strain of ASM tissue strips from asthmatic and non-asthmatic subjects has found that ASM from asthmatic subjects are more resistant to mechanical perturbation. This suggests that asthmatic and non-asthmatic ASM is intrinsically different and that this difference may lie in the ability to preserve the integrity of subcellular force-generating structures during length oscillation.

As discussed above, the mechanism(s) underlying the ability of ASM to maintain force is not entirely clear. The ASM's ability to maintain stiffness may be related to its ability to maintain force, because the former reflects the property of a more robust subcellular structure. It is not known whether there is a difference between asthmatic and non-asthmatic ASM in terms of their passive stiffness and sensitivity to calcium and Rho-kinase activity. Lan et al (2015) have shown that the maintenance of active force in an isometric contraction is compromised when Rho-kinase is inhibited. When strips are subjected to oscillatory strain, the same degree of Rho-

kinase inhibition leads to a much greater decline in force maintenance compared to that under isometric conditions. This indicates a synergistic effect of oscillatory strain and Rho-kinase inhibition on the ability of the ASM to maintain force. A similar synergy has been observed by Ansell et al (2014) in bronchial segments subject to oscillatory pressure. They found that the combination of isoprenaline and oscillatory pressure reduced airway wall stiffness (presumably due to the action of isoprenaline on ASM) and resulted in a much greater reversal of airway narrowing compared with static conditions.

A better understanding of the mechanisms underlying force development and maintenance will allow us to more accurately identify drugs targeting specific aspects of ASM function (or dysfunction). One should keep in mind that ASM in vivo functions in a mechanically dynamic environment and that ASM force and stiffness are differentially affected by the mechanical perturbation. Reducing muscle stiffness may be an effective way to prevent excessive narrowing of the airways because it allows the oscillatory strains associated with tidal breathing and DI to more effectively exert their bronchodilatory and bronchoprotective effects. Furthermore, identifying protein substrates downstream of the Rho-kinase pathway responsible for regulating cytoskeletal stiffness may allow us to develop specific drugs with less side effects (compared with those targeting upstream kinases like Rho-kinase) to treat airway hyperresponsiveness in asthma.

1.5   Summary of thesis research

The focus of my research throughout my Masters program has been to improve the current understanding of mechanisms of ASM contraction, specifically the roles of actomyosin interaction in force development and the roles of the cytoskeletal network in force maintenance.

Chapter 2 focuses on selective activation of cytoskeletal components within the ASM cells while avoiding activation of the actomyosin cross-bridge cycle. This was achieved by removing enough calcium within the cells so MLC20 phosphorylation was absent. We hypothesize that there is a calcium independent activation of ASM which is caused by activation

of the dynamic cytoskeleton. Our aims were to examine the mechanical manifestations of this selective activation both biomechanically and biochemically. Results presented in this chapter have not been published. However, they laid the foundation for a more extensive study in the future.

In chapter 3 the biphasic response of ASM subjected to a ramp stretch was described. Stretches with different amplitudes and velocities were applied to ASM. Also stretches occurred at different time points during contraction, at different degrees of activation, and in the presence and absence of enzyme inhibitors. The corresponding biphasic responses provided evidence to suggest that the initial phase of response stems mainly from the attached cross-bridges whereas the later phase contains information about the structural remodelling of the cytoskeleton and how the remodelling process was influenced by activation time and activities of enzymes such as Rho-kinase and PKC. A manuscript based on this chapter has been accepted for publication in the American Journal of Physiology – Lung Cellular and Molecular Physiology.

Chapter 2   Zero-calcium activation in ASM

2.1   Introduction

In asthmatics, the airways are stiffer even when the airway smooth muscle (ASM) is not contracted (Colebatch, Finucane, and Smith 1973). This could be due to airway remodelling and the accompanying fibrotic changes in airway components external to ASM layer. However, ASM contribution to passive airway stiffness has not been ruled out. Airway stiffness consists of many components, but has typically been classified as having an active component from ASM (cross-bridge activation) and passive components (non-cross-bridge muscle components, and other components of the airway). Recently, a new contributor to ASM stiffness has been identified, stemming from ASM but lying within the so-called passive component, as it resides outside the active component that involves cross-bridge activation (Raqeeb et al. 2012). This study indicates that an element of passive stiffness may actually be active in the sense that it is intracellular in origin and that it is regulated by an intracellular signalling network, and interestingly it has both a calcium dependent and independent component (Raqeeb et al. 2012; Lan et al. 2013).

The commonly known role of calcium in smooth muscle cells is initiating contraction. Calcium is integral in permitting the interaction of actomyosin in the so called cross-bridge cycle by activating the myosin light chain kinase (MLCK) which phosphorylates the myosin regulatory chain (MLC20) (Frearson, Focant, and Perry 1976; A. Sobieszek 1977). Other mechanisms independent of calcium also regulate cross-bridge activation. For example, a mechanism that does not directly phosphorylate the MLC20, but causes an increase in its phosphorylation during activation, is a phenomenon called calcium sensitization (Kitazawa and Somlyo 1991). Proteins such as Rho-kinase (Uehata et al. 1997; Somlyo and Somlyo 2003) and Protein kinase C (PKC) (Masuo et al. 1994; Somlyo and Somlyo 2003) are involved with calcium sensitization, and do so by inhibition of the myosin light chain phosphatase (MLCP). There has also been mechanisms identified which phosphorylate the cross-bridges in calcium depleted smooth muscle cells (Ishihara et al. 1989; Obara et al. 1989; Niiro and Ikebe 2001). Here, cross-bridge cycling occurs because of MLC20 phosphorylation, and may occur due to the inhibition of phosphatases.

Outside of the contractile domain where cross-bridges reside, an integral component necessary for smooth muscle contraction is the cytoskeleton. Studies have shown that inhibition of the dynamic process of cytoskeletal remodelling causes a decrease in smooth muscle contraction, without affecting the phosphorylation of the MLC20 (Tang, Turner, and Gunst 2003; Zhang et al. 2005). The regulation of the cytoskeleton is complex, as it encompasses many proteins and overlaps with many other pathways (Susan J. Gunst and Zhang 2008; Zhang, Huang, and Gunst 2012); however, the pathways seem to be largely independent of regulation by calcium. One of the mechanisms of the cytoskeleton is anchoring the actin filaments to membrane adhesion sites (Zhang, Huang, and Gunst 2012; Opazo Saez et al. 2004). It is unknown whether connections within the cytoskeleton to adhesion sites contribute to the stiffness of smooth muscle. A recent study has shown that stiffness of ASM increases in the absence of cross-bridge activation, raising the possibility that an increase in stiffness may be due to cross-linking of the cytoskeletal filaments (Lan et al. 2013). Since it appears that cytoskeletal activation occurs independent of calcium, it may be reasonable to believe that the dynamic cytoskeleton is responsible for calcium independent passive stiffness.

This study aimed to examine the activation of ASM in a calcium free environment. Sheep tracheal ASM strips were used to test biomechanical changes upon activation, all of which are independent of the active cross-bridge cycle as calcium was not present. The study also aimed to examine Rho-kinase's involvement in calcium-independent ASM function, as the kinase is a known mediator in the regulation of properties of active cytoskeleton (Amin et al. 2013; Zhang, Huang, and Gunst 2012), and potentially passive stiffness. Also in this study, preliminary data were collected to identifying potential proteins downstream of Rho-kinase responsible for the calcium-independent development of force and stiffness in ASM. Identification of these proteins would be an important first step in the development of a new class of anti-asthma drugs that target passive airway stiffness rather than the conventional target of active force.

2.2   Methods

2.2.1   Tissue preparation and equilibration

Sheep tracheas were obtained from a local abattoir with approval from the Animal Care Committee and Bio-safety Committee of the University of British Columbia. The tracheas were immediately put into Krebs solution (pH 7.4; 4°C; 118 mM NaCl, 4 mM KCl, 1.2 mM NaH_2PO_4, 22.5 mM $NaHCO_3$, 2 mM $CaCl_2$ and 2 g/l dextrose) after removal from the animals. The in situ length of the tracheal muscle was recorded prior to cutting the C-shaped cartilage ring and was used as a reference length (L_{ref}) for normalization of length measurements. Upon isolation of the smooth muscle strip, adventitial connective tissue and the epithelial and sub-epithelial layers were removed. The dissection resulted in tissue strips of approximately 7 mm long, 1.5 mm wide, and 0.3 mm thick. Clips made of aluminum foil were then attached to each end of the strip (length wise), allowing for the strip to be connected to a dual-mode muscle lever system (Aurora Scientifics, Aurora, ON) that simultaneously measures changes in force and length. The length resolution is 1 μm; the force resolution is 0.3 mN; the length step response time is 1 ms; the force step response time is 1.3 ms. The tissue was submerged in an organ bath filled with Krebs solution maintained at 37°C and aerated with carbogen containing 95% O_2 and 5% CO_2.

To allow the muscle to recover from cold storage and trauma during dissection, the dissected strip was set to L_{ref} and stimulated for 9 s once every 5 min with an electrical field stimulation (EFS) (60 Hz AC, voltage 15-25 V). The Krebs solution in the organ bath was replaced by fresh, aerated Krebs solution at 37°C for each cycle. The tissue was deemed equilibrated once it reached a stable maximal isometric force (F_{max}) and a stable low resting tension. No strip with resting tension higher than 2% F_{max} was used for this study.

2.2.2   Removal of Calcium in the ASM tissue

After equilibration, the Krebs solution was replaced with zero-calcium Krebs solution. The zero-calcium solution contains the same ingredients as normal Krebs solution plus three chemicals that act to remove calcium from the cytoplasm of ASM cells: EGTA (2 mM), A23187

(20 µM), and Cyclopiazonic acid (CPA) (10^{-5} M). EGTA acts as a chelating agent for calcium, binding to free calcium in the cytoplasm. A23187 is a Calcium Ionophore that allows for the passage of calcium ions across membranes. CPA is a sarco/endoplasmic reticulum Ca^{2+}-ATPase (SERCA) pump inhibitor; it prevents the pump from transporting calcium released into the cytoplasm back into the SR. While being incubated in the zero-calcium solution, the tissue was stimulated with EFS every five minutes for 30 minutes (total of six stimulations). Active force declined with each stimulation. After 30 min, the tissue produced no active force, suggesting the intracellular calcium had been reduced to a level below the physiological requirement to activate the cross-bridges.

2.2.3   Force and stiffness measurements

Post calcium removal, the muscle was stimulated with ACh (10^{-5} M), and the force was measured. A plateau of force developed approximately 120 s after the onset of stimulation (F_{max}). To assess stiffness of the stimulated muscle in zero-calcium solution, a quick step-stretch of 8% at a speed of 0.8% L_{ref} per ms. The change in force due to the stretch divided by the stretch amplitude was taken as a measure of the muscle stiffness (S_{max}) (Figure 2.1).
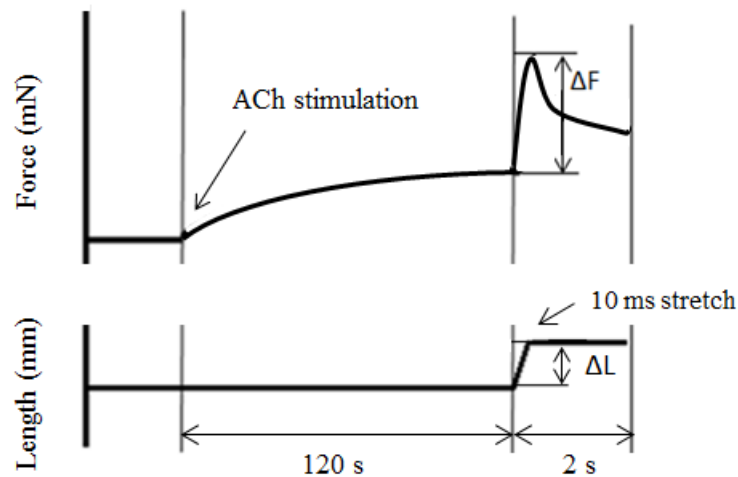
Figure 2.1 Graphic illustration of ACh activation of ASM in zero calcium with a stretch to measure ASM stiffness. The ratio of ΔF/ΔL is taken as an index of stiffness (S_{max}).

2.2.4 Measurement of phosphorylation of the regulatory myosin light chain (MLC20)

ASM strips post equilibration and calcium removal were snap frozen with pre-chilled acetone (-78℃). Tissues were frozen under various conditions. The frozen tissue samples were put in eppendorf tubes and submerged in 5% trichloroacetic acid (TCA) and 10 mM dithiothreitol (DTT) and stored in -80℃ until protein extraction was performed.

For protein extraction, tissue strips were homogenized in extraction buffer (6.4 M urea, 10.0 mM DTT, 10.0 mM EGTA, 1.0 mM EDTA, 5.0 mM NaF, 1.0 mM phenylmethylsulfonyl fluoride, 26.3 mM Tris base, and 28.6 mM glycine). Approximately 150 μg of extraction buffer was added to 1 mg of wet tissue. The tissue was then sonicated on ice and then centrifuged at 13200g for 30 minutes at 4℃. The supernatant was collected. Protein quantification was done by Bradford protein assay (Quick Start Bradfrod Protein Assay; BioRad, Mississauga, Ontario, Canada). The tissue was stored at -80℃.

To determine the phosphorylated and non-phosphorylated MLC20, electrophoresis and western blot was used. A 10% glycerol nondenaturing mini-gel with 3% acrylamide-urea stacking gel was performed. Supernatant from the six conditions were loaded in equal protein quantity per lane. Electrophoresis at 200 V for 2.5 hours at room temperature was used to separate the protein. The running buffer contained 100 mM glycine, 50 mM Tris, and β-mercapoethanol at 1.0 mL per L of buffer. Proteins were transferred to 0.2 μm nitrocellulose membrane at 25 V, overnight at 4 ℃. Blocking was done with TBS – 5% BSA at room temperature for 1 hour.

Western immunoblots allowed for measurement of MLC20p/MLC20total. A monoclonal mouse antibody to smooth muscle MLC20 (clone MY-21; Sigma-Aldrich, Oakville, Ont.) 1:5,000 and a goat antimouse IRDye 800 conjugated antibody (Rockland, Gilbertsville, Pennsylvania, USA) 1:10,000. Between the first and secondary antibodies, and after the secondary antibody, the membrane was washed 4 times every 5 minutes with TBST-5%BSA. A LI-COR Odyssey 2.1 Infrared Imaging System (Lincoln, Nebraska, USA), scanned the membrane and quantified the intensity. Background intensity was subtracted out by the software.

2.2.5   Inhibitor effect on zero-calcium activation

To investigate the mechanism behind zero-calcium activation, the Rho-kinase and PKC pathways were inhibited and changes to biomechanics were measured. Strips were incubated in H1152 (Torcris Bioscience), a Rho-kinase inhibitor for 30 min at 3 µM. Also GF109203x (Enzo Biochem), a PKC inhibitor was incubated for 50 min at 10 µM. H1152 was added to strips already exposed to activation and then relaxed. PKC inhibition was compared to a time control and normalized to its time control value.

2.2.6   Kinexus analysis of proteins involved with zero-calcium activation

To identify potential proteins involved with the zero-calcium activation, an 18 protein western blot service provided by Kinexus Bioinformatics Corporation was used. 17 antibodies were selected from the list of Kinexus antibodies, one was provided by us (MLC20). A focus of was on proteins within the SM field found to be involved in cytoskeletal dynamics. Tissue preparation for Kinexus was done by the following protocol. Two conditions (5 and 6 on figure 2.4) consisted of four strips from four different tracheas pooled together for each condition. Protein extraction was done prior to shipment of samples. Protocol and lysis buffer for extraction was provided by the company and can be found in the information package (KCPS 1.0). Protein phosphorylation counts were done via chemiluminensce. In order to compare the two conditions, a coefficient was derived from the results in order to standardize the values.

2.2.7   Statistics

All stats were performed in sigma plot using either paired or unpaired t-tests. The data is presented as means±SE. n is used to indicate the number of tracheal muscle preparations from different sheep. A p value of .05 or less was used to reject the null hypothesis.

2.3   Results

2.3.1   Force and stiffness

Figure 1 shows force increase after 120 s of ACh stimulation in zero-calcium Krebs solution. Compared to that in the relaxed zero-calcium state, the ACh-activated tissue in zero-calcium solution produced significantly higher force ($323 \pm 48\%$, $p = 0.010$, $n = 5$). Figure 2 shows changes in tissue stiffness assessed by an 8% L_{ref} stretch in zero-calcium solution with and without ACh. The stiffness increased significantly when ACh was present ($170 \pm 17\%$, $p < .001$, $n = 6$). Stiffness values in Fig. 2.2 and 2.3 were expressed as normalized values, i.e., % of the stiffness in the relaxed state. The absolute values for force and stiffness in the relaxed state were $1.25 \pm .428$ (mN) and 11.98 ± 1.70 mN/mm, respectively.

2.3.2   MLC20 phosphorylation

The results of quantification of MLC20 phosphorylation is shown in Figure 2.4. Densitometry were carried out for the 6 lanes each with one band representing phosphorylated MLC20 and one lane representing total MLC20. The ratios were plotted. Lanes 1 and 2 show the controls in normal Krebs in the relaxed and calcium activated states, respectively. Under these conditions, phosphorylation of MLC20 increased from 5% in the relaxed state to 50% in the activated state 120 s after ACh application. Lanes 3 – 6 representing conditions under which calcium had been removed and all showed no phosphorylation of MLC20 in the relaxed and activated (120 s) states. Specifically, lanes 5 and 6 showed results from zero-calcium conditions where intracellular calcium had been removed using calcium Ionophore, CPA, and EGTA. This method led to the same result as that in lanes 3 and 4 which was obtained from a less rigorous method of calcium removal. The protocol for conditions 5 and 6 were used for the remaining experiments.

2.3.3 Inhibition of Rho-kinase and PKC

Rho-kinase inhibition abolished nearly all of the active force induced by ACh activation under zero-calcium conditions. The force development in the control group (zero-calcium plus ACh) was 2.5 mN; the developed force was abolished in the test group (zero-calcium plus ACh and 3 μM H1152, Figure 2.5). The results are significantly different (n=3, p=.047).

PKC inhibition (10 μM GF109203x) did not result in a change in force of activation (n= 3, p>0.05, Fig. 2.6). The control was normalized to a time control, to take into account possible changes in force over the 50 min incubation time. The result indicated no change of tissue contractility over the incubation period. The protocol for the test group (with PKC inhibitor) also included a time control (value given as F_{max}).

2.3.4 Kinexus results of phosphorylated proteins

18 proteins were selected to screen for the level of phosphorylation under zero-calcium conditions in the presence and absence of ACh (10^{-4} M) (Table 2.1). The criteria for the selection were based on the consideration of possible roles played by the proteins in force development and force maintenance in smooth muscle. Out of the 18 proteins, 9 were detected to be phosphorylated, and 9 had no detectable levels of phosphorylation (Figure 2.7). Some proteins were found to increase phosphorylation with ACh activation; e.g., caldesmon (105) by 34%, cortactin by 75%, integrin b by 125%, and vimentin by 309%. Other proteins were found to decrease phosphorylation with ACh activation, such as adducin gamma by 35%, and PKC delta by 39%.

FULL NAME OF PROTEIN	ABBREVIATION
Adducin alpha (ADD1) [S726]	Adducin a
Adducin gamma (ADD3) [S693]	Adducin g
Caldesmon [S789] (105)	Caldesmon
Caldesmon [S789] (75)	Caldesmon
Caveolin 2 [S36]	Caveolin 2
Cofilin 2 [S3]	Cofilin 2
Cortactin (amplaxin) (mouse) [Y466]	Cortactin
Focal adhesion protein-tyrosine kinase [S722]	FAK
Heat shock 27 kDa protein beta 1 (HspB1) [S82]	Hsp27
Integrin beta 1 (fibronectin receptor beta subunit, CD29 antigen) [S785]	Integrin b1
LIM domain kinase 1 [Y507+T508]	LIMK1
LIM domain kinase 2 [Y504+T505]	LIMK2
Mitogen-activated protein kinase-activated protein kinase 2 [T222]	MAPKAPK2
Myosin Light Chain 20 [S19]	MLC20
Paxillin 1 [Y118]	Paxillin 1
Paxillin 1 [Y31]	Paxillin 1
Phosphatidylinositol-3,4,5-trisphosphate 3-phosphatase and protein phosphatase and tensin homolog deleted on chromosome 10 [S380/T382/T383]	PTEN
Protein-serine kinase C delta [S664] (75)	PKCd
Protein-serine kinase C delta [S664] (79)	PKCd
Protein-serine kinase C epsilon [S729]	PKCe
Protein-serine kinase C theta [S695]	PKCt
Ras-related C3 botulinum toxin substrate 1 [S71]	Rac1/cdc42
Vimentin [S34]	Vimentin

Table 2.1 List of 18 proteins and abbreviations from Kinexus study. Phospho-site name included in square brackets.
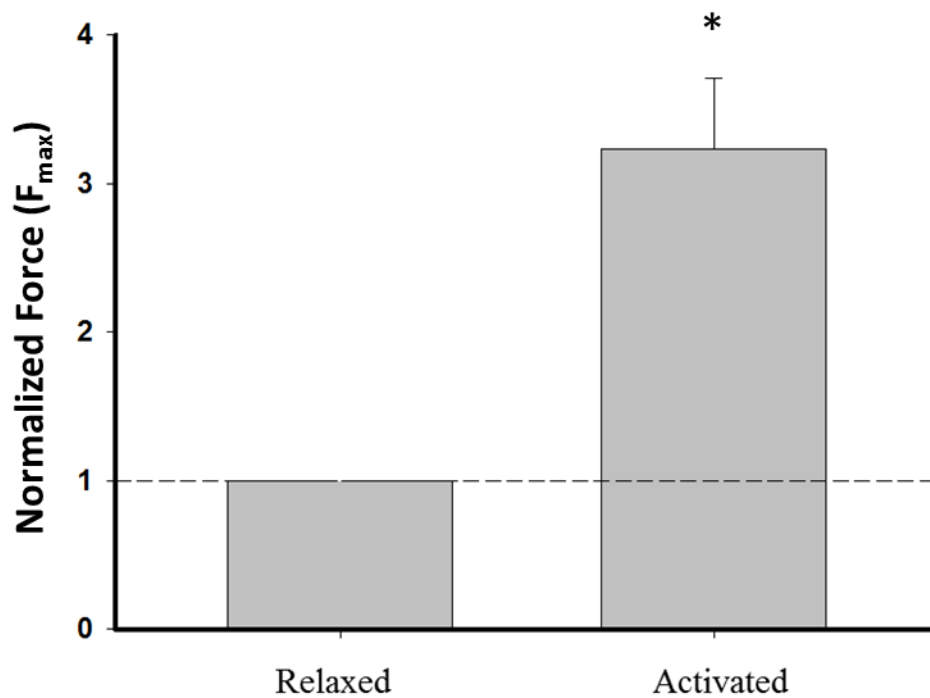
Figure 2.2 Force development in ASM tissue activated with ACh in zero-calcium krebs.

Control (un-activated) group versus ACh 10^{-5} M (activated 120 s) group. Both groups were normalized to the control value. The control value represents a time control, the change in force over 120 s of no activation. Activated group is significantly different (p=.010, n=5), paired t-test.
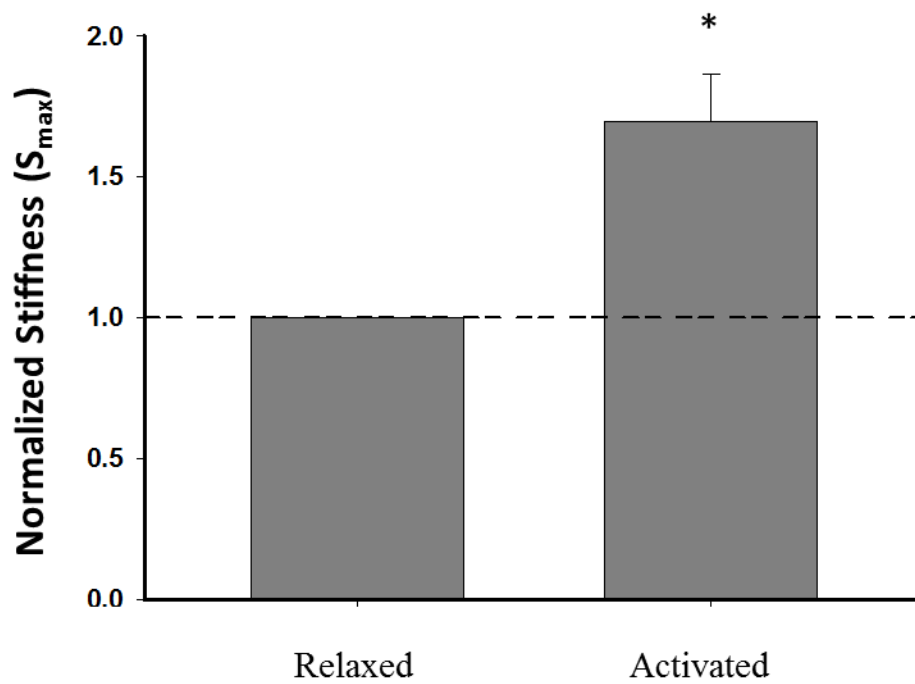
Figure 2.3 Stiffness of relaxed and activated (10^{-5} M) ASM in zero-calcium krebs. A quick stretch (of amplitude 8% L_{ref} and of speed 0.8% L_{ref}/ms) was applied to ASM strips before (Relaxed) and 120 s after ACh activation (Activated). The values for the activated stiffness were normalized to the control stiffness (relaxed zero-calcium). The activated stiffness is significantly different from than the control stiffness (p <.001, n=6) paired t-test.
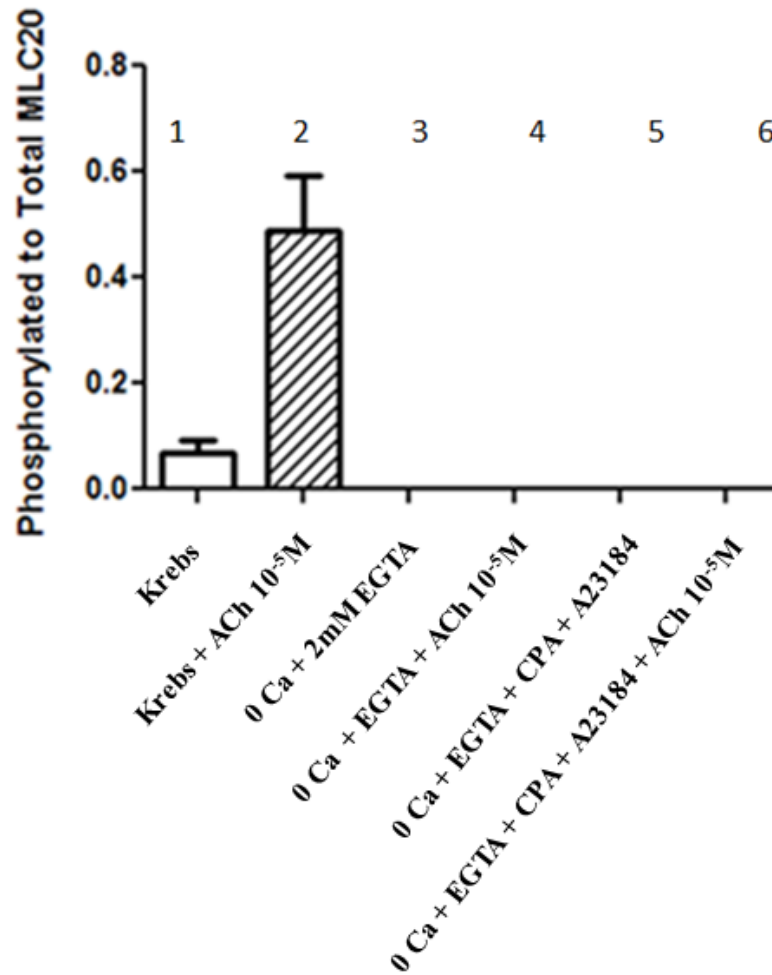
Figure 2.4 MLC20 phosphorylation under various conditions. The ratios of phosphorylated MLC20 over the total MLC20 were plotted. In the normal calcium control groups (1 and 2), calcium was not removed. Basal phosphorylation is shown in 1 (relaxed); ACh-induced phosphorylation in 2. In conditions 3 (relaxed) and 4 (activated), calcium was removed with 2 mM EGTA. In conditions 5 (relaxed) and 6 (activated), calcium was removed with 2 mM EGTA, 10^{-5} M CPA, and 20 μM A23187. n=4 for each group.
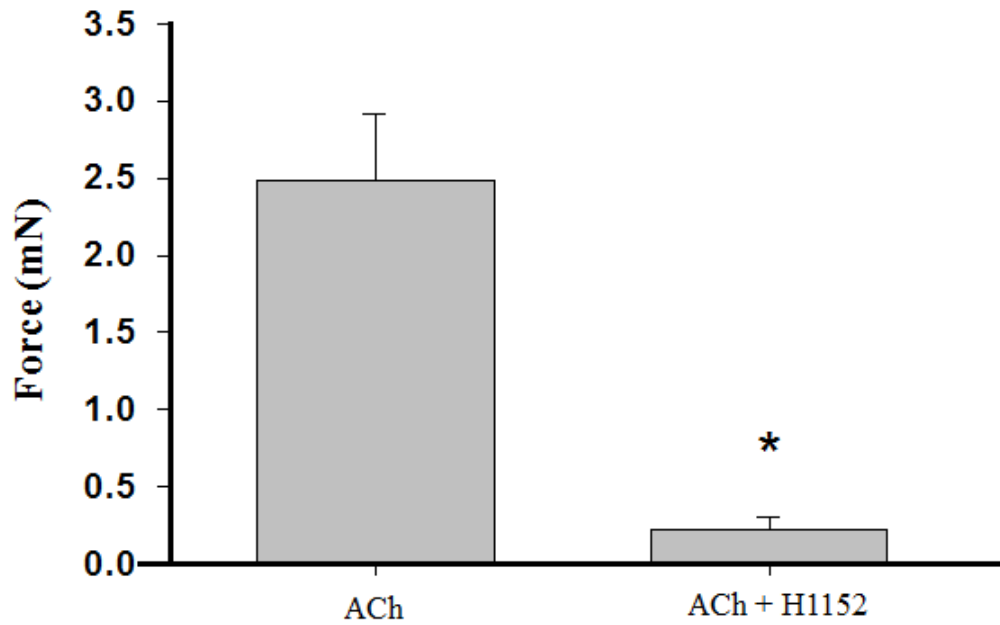
Figure 2.5 Rho-kinase inhibition in zero-calcium activation. Force generation after 120 s stimulation by ACh (10^{-5} M) in the control (ACh only) and test (ACh plus H1152) groups. *, significant difference (n=3, p=.047) by paired t-test.
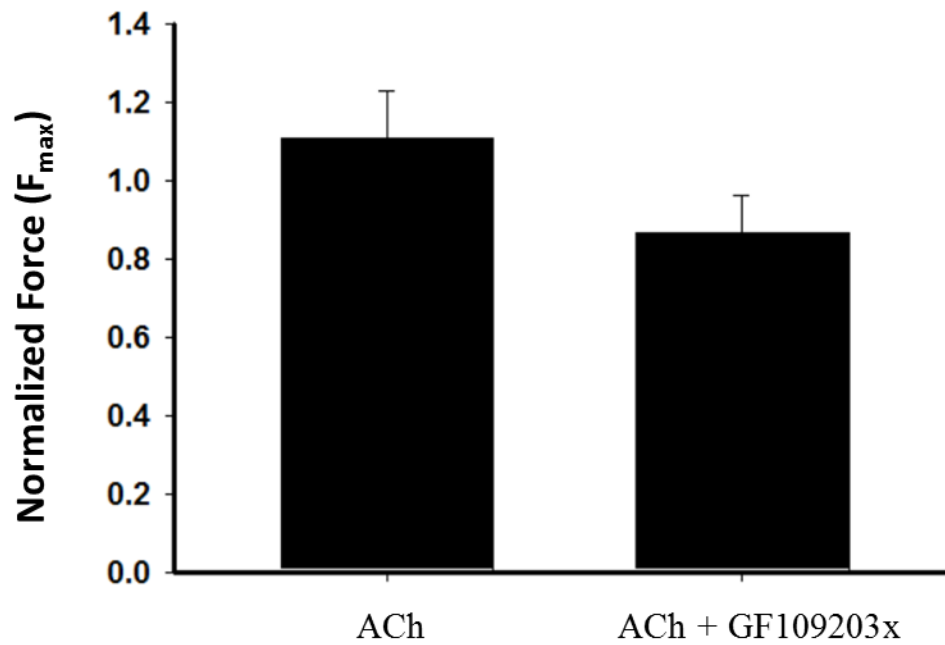
Figure 2.6 PKC inhibition in zero-calcium activation. Force generation after 120 s stimulation by ACh (10^{-5} M) in the control (ACh only) and test (ACh plus GF109293x) groups. The results are not significantly different (n=4, p=.343) by t-test.
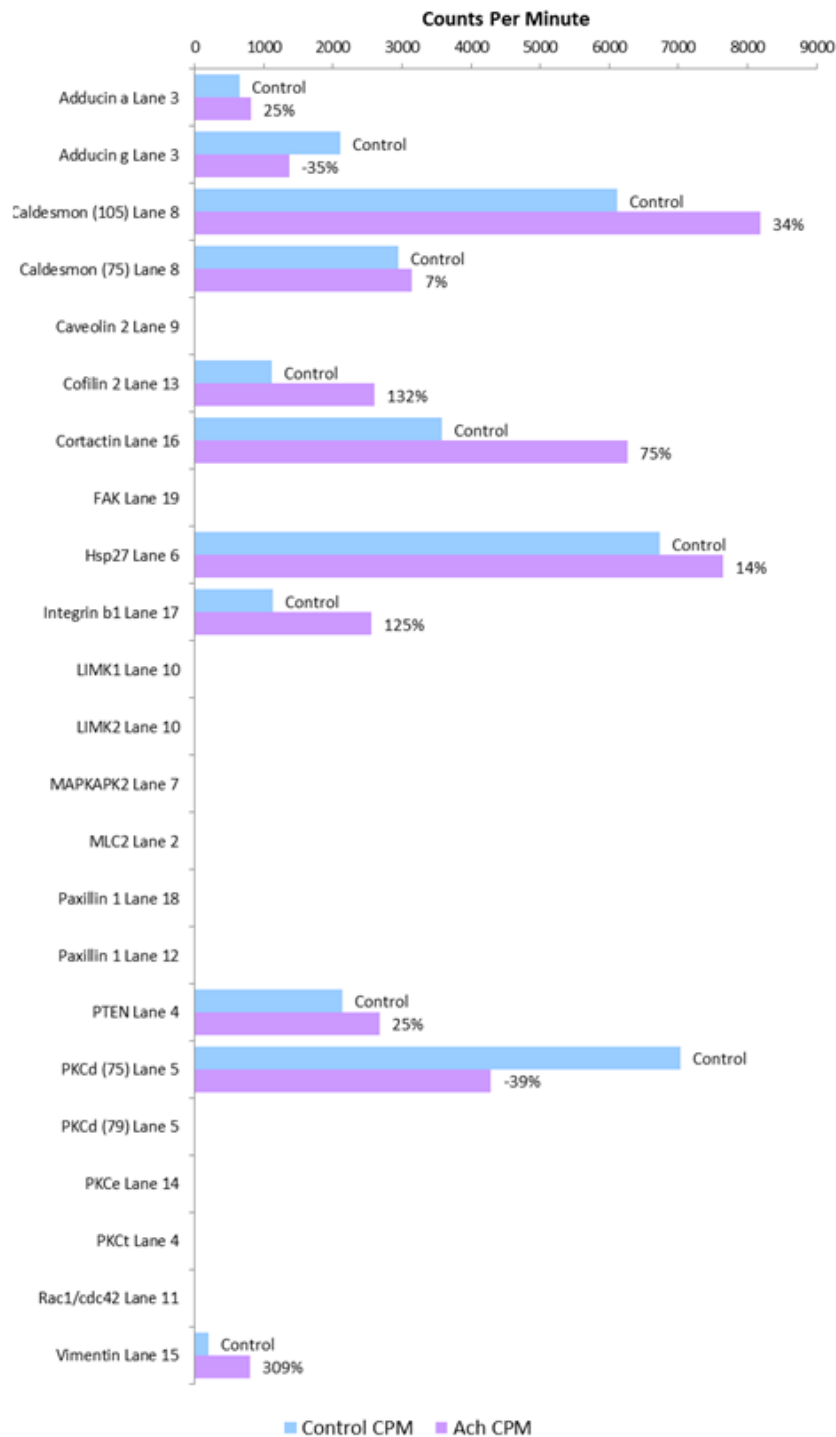
Figure 2.7 Kinexus preliminary results for 18 selected proteins. Control (relaxed) in blue, ACh (10^{-4} M) activated group in purple. Counts per minute (CPM) of detected chemiluminescence was used to indicate the level of phosphorylation. Some of the antibodies used detected multiple protein subtypes (i.e., LIMK1 and LIMK2), thus more than 18 proteins measurements were listed. The lysates for each condition consisted of 4 different tracheas pooled together. There were no technical repeats done.

2.4   Discussion

The most important findings described in this chapter are 1) ACh stimulation is able to cause force and stiffness to increase in ASM tissue even in the absence of free calcium and MLC20 phosphorylation; and 2) inhibition of Rho-kinase but not PKC abolishes force development induced by ACh under a zero-calcium condition. This suggests that the calcium-independent force development in ASM is regulated by Rho-kinase.

One advantage of studying ASM in a calcium free environment is that it allows for the activation of calcium-independent signalling pathways in the cells while avoiding activation of calcium-dependent pathways such as phosphorylation of the MLC20 that turns on the cross-bridge cycle.

ACh binds to ASM cells via the muscarinic 3 (M3) receptors, activating the G-protein dependent signalling pathways (Somlyo and Somlyo 2003; Puetz, Lubomirov, and Pfitzer 2009). Through the G-protein signalling cascade, proteins such as RhoA are activated and in turn it activates Rho-kinase, leading to the activation of downstream pathways that Rho-kinase mediates (Puetz, Lubomirov, and Pfitzer 2009). One branch of the pathways Rho-kinase is known to regulate mediates the structural remodelling of cytoskeleton and modulates cytoskeletal dynamics in cell motility (Amano, Nakayama, and Kaibuchi 2010). Although not many studies have been done investigating the roles of Rho-kinase in altering mechanical properties of cytoskeleton in smooth muscle, recent studies clearly indicated that Rho-kinase was involved (Raqeeb et al. 2012; Lan et al. 2013; Lan et al. 2015).

The mechanism underlying the stiffening and slight increase in force seen in ASM strips stimulated by ACh in zero-calcium bathing solution (Fig. 2.2 and 2.3) is not entirely clear. However, it is clear that the force and stiffness development occurred in the absence of MLC20 phosphorylation (Fig. 2.4). This suggests that the cycling myosin cross-bridges normally responsible for force and stiffness development in calcium-dependent contractions are not likely the source for the calcium-independent force and stiffness, because the prerequisite for the activation of these cross-bridges is MLC20 phosphorylation (Puetz, Lubomirov, and Pfitzer

2009). One potential candidate responsible for the calcium-independent force and stiffness is the putative cross-linkers of cytoskeletal filaments (Lan et al. 2015). Linking of adjacent cytoskeletal filaments by cross-linkers may cause a slight structural change in the cytoskeleton; this would explain the slight increase in force (Fig. 2.2). The increase in stiffness (Fig. 2.3) is another line of evidence for the existence of cross-linkers.

The function of the cross-linkers (or whatever structural components responsible for the calcium-independent force and stiffness) does not depend on MLC20 phosphorylation (Fig. 2.4), but it is dependent on activation of the Rho-kinase (Fig. 2.5), and interestingly not dependent on activation of PKC (Fig. 2.6). It should be pointed out that the Rho-kinase activity observed in Fig. 2.5 is calcium independent, but regulated by the signalling network involving M3 receptor activation by ACh. So far we do not know what enzymes and proteins up and down stream of Rho-kinase are involved in the development of the calcium-independent force and stiffness.

In an attempt to elucidate the signalling network for the calcium-independent regulation of force and stiffness in ASM, we carried out a preliminary study using the service provided by Kinexus. 17 proteins were selected from a Kinexus panel of antibodies, one was provided by our laboratory as a control to match our results from Figure 2.4 (MLC20). The criteria for selecting the 17 proteins were based on known cytoskeletal proteins that are likely candidates to function as cross-linkers and regulated through phosphorylation by enzymes.

Although the Kinexus results (n=1) show promise, it is preliminary and therefore inappropriate to make any conclusions based on the data. The high cost of Kinexus service prevented us from repeating the experiments. However, the preliminary results did provide some useful information. Examination of the results (Fig. 2.7) showed that the data indeed fit into some of the current literature of SM cytoskeletal dynamics during contraction. For instance, cortactin phosphorylation increased during activation; this agrees with the finding by Wang et al demonstrating cortactin's role in regulating actin polymerization during ASM contraction (R. Wang et al. 2014). Specifically, the authors found that during contraction cortactin was phosphorylated and this in turn aided actin polymerization. Integrin beta is another protein that has sparked a lot of interest in the activation of the cytoskeleton in ASM. This trans-membrane

protein is the site of focal adhesion in smooth muscle cells, where it tethers the cytoskeleton through the cell membrane to the extracellular matrix (Gerthoffer and Gunst 2001). It also plays an active role in actin polymerization during contraction. Again, the result in Fig. 2.7 is consistent with the known mechanisms of integrin beta, and is a potential mechanism behind the calcium-independent activation in smooth muscle. A final protein to mention here that was phosphorylated in the activated zero-calcium condition is cofilin, which contradicts some literature presently known about the protein. Cofilin is known to be dephosphorylated when activated, and when activated its function is to excise actin filaments, depolymerizing the filamentous chain (Kiuchi et al. 2007). In ASM, one experiment has shown that cofilin is dephosphorylated during contraction, allowing actin to reorganize and permit a sustained contraction (Zhao et al. 2008). The authors argue that it is the activation of cofilin that permits the remodelling of actin filaments, which is a necessary process for ASM contraction. Other studies have shown that the activation of Rho-kinase regulates the LIM-kinase pathway, which in turn inactivates cofilin (phosphorylates) permitting cytoskeletal reorganization, as the actin is now stable (Fukata, Amano, and Kaibuchi 2001). Our data is more in line with the latter findings, if we assume actin polymerization is associated with the increase in stiffness.

Validation of the Kinexus results is necessary to confirm the identities of the proteins being phosphorylated or dephosphorylated (turned on/off) during activation. Further extensions to this work would include testing the effect of H1152 (Rho-kinase inhibitor) to determine if phosphorylation of the proteins changes. The results could lead to two possible findings: proteins responsible for mediating the ACh induced zero-calcium activation and proteins downstream of the Rho-kinase pathway. The findings will be invaluable to the understanding of calcium-independent regulation of force and stiffness development in ASM.

Recent studies in ASM research have highlighted passive stiffness as a potential cause of reduced airway distensibility seen in asthmatics (Raqeeb et al. 2012; Pyrgos et al. 2011; Chun Y. Seow 2013; Lan et al. 2013). Elucidation of signalling pathways regulating calcium-independent force and stiffness in ASM will greatly facilitate our effort in identifying enzymes and proteins that could be targeted in asthma therapy.

2.5   Conclusion

This research can be appreciated from two angles. First, from a basic science perspective, we have introduced a way to activate ASM contraction outside the classical calcium-dependent mechanism of actomyosin interaction. The preliminary studies described in this chapter have paved the way for future studies to examine the signalling pathways responsible for calcium-independent activation and stiffening of ASM. Second, from the perspective of asthma pathology and airway distensibility, this research is a first step in identifying new potential targets for reversing stiffened airways in asthma therapy.

Chapter 3   Biphasic force response to iso-velocity stretch in airway smooth muscle[2]

3.1   Introduction

Oscillatory strain is experienced by airway smooth muscle in vivo during tidal breathing and deep inspiration, and it modulates the muscle's contractility (S. J. Gunst 1983). Small amplitude oscillation perturbs actomyosin interaction and reduces the muscle's ability to generate and maintain force (Mijailovich, Butler, and Fredberg 2000), whereas large amplitude oscillations not only disrupt actomyosin interaction, but also induce cytoskeletal remodelling (Fredberg et al. 1999; Oliver et al. 2010). Although reorganization of the cytoskeleton is believed to play a key role in smooth muscle contraction, the molecular mechanism underlying the strain induced structural change is largely unknown. To gain insight into the mechanism, a better characterization of the strain-dependent force response from the muscle may be needed. Force response from an activated muscle to a relatively slow rate of strain likely originates from two sources, the attached actomyosin crossbridges and the cytoskeleton stiffened by cross-linkers connecting adjacent cytoskeletal filaments (Donovan et al. 2010; Lan et al. 2015). Differentiation of the contributions of the two sources to the force response will be an important step in isolating the component of the force response associated with cytoskeleton and a first step in unravelling the signalling pathways regulating cytoskeletal structural change.

In skeletal muscle, force response to an iso-velocity (ramp) stretch has been well characterized. Force increases rapidly during the initial phase of stretch followed by a slower increase in force in the later phase of stretch, with the two phases clearly separated by a distinct transition point (Edman 1999; Getz, Cooke, and Lehman 1998; Lombardi and Piazzesi 1990; Pinniger, Ranatunga, and Offer 2006). It is thought that during the initial phase the attached actomyosin crossbridges are being stretched, and the transition point marks the critical strain where detachment of the crossbridges occurs. Furthermore, force maintenance during the later

---

[2] A version of this chapter has been published. Brandon A. Norris, Bo Lan, Lu Wang, Christopher D. Pascoe, Nicholas E. Swyngedouw, Peter D. Paré, and Chun Y. Seow. Biphasic force response to iso-velocity stretch in airway smooth muscle. *AJP Lung* - 2015.

phase is thought to be due to rapid reattachment of some detached crossbridges (Getz, Cooke, and Lehman 1998; Lombardi and Piazzesi 1990) and also due to stretching of a non-crossbridge, parallel elastic element that stiffens upon muscle activation (Pinniger, Ranatunga, and Offer 2006).

The biphasic force-response to ramp stretch has also been observed in smooth muscle (Meiss 1987). Although the crossbridge mechanism used to explain the phenomenon in skeletal muscle (Edman 1999; Getz, Cooke, and Lehman 1998; Lombardi and Piazzesi 1990; Pinniger, Ranatunga, and Offer 2006) could be applied to smooth muscle, a non-crossbridge mechanism such as cytoskeletal stiffening has never been explored in smooth muscle. In the present study force-response to a ramp stretch in airway smooth muscle was examined under different experimental conditions to identify crossbridge and non-crossbridge (cytoskeletal) sources of stiffness, and to discern how the stiffness varied during the different phases of a ramp stretch. The results are discussed in the context of muscle performance in the mechanically dynamic lung/airway environment and with respect to possible interventions that could reduce the ability of airway smooth muscle to contract and maintain force in the airways of asthmatic patients.

3.2   Materials and methods

3.2.1   Tissue preparation and equilibration

Sheep tracheas were obtained from a local abattoir with approval from the Animal Care Committee and Bio-safety Committee of the University of British Columbia. The tracheas were immediately put into Krebs solution (pH 7.4; 4°C; 118 mM NaCl, 4 mM KC, 1.2 mM NaH_2PO_4, 22.5 mM $NaHCO_3$, 2 mM $CaCl_2$ and 2 g/l dextrose) after removal from the animals. The in situ length of the tracheal muscle was recorded prior to cutting the C-shaped cartilage ring and was used as a reference length (L_{ref}) for normalization of length measurements. Upon isolation of the smooth muscle strip, adventitial connective tissue and the epithelial and sub-epithelial layers were removed. The dissection resulted in tissue strips approximately 7 mm long, 1.5 mm wide, and 0.3 mm thick. Clips made of aluminum foil were then attached to each end of the strip (length wise), allowing for the strip to be connected to a dual-mode muscle lever system (Aurora

Scientifics, Aurora, ON) that simultaneously measures changes in force and length. The length resolution is 1 μm; the force resolution is 0.3 mN; the length step response time is 1 ms; the force step response time is 1.3 ms. The tissue was submerged in an organ bath filled with Krebs solution maintained at 37℃ and aerated with carbogen containing 95% O_2 and 5% CO_2.

To allow the muscle to recover from cold storage and trauma during dissection, the dissected strip was set to L_{ref} and stimulated for 9 s once every 5 min with an electrical field stimulation (EFS) (60 Hz AC, voltage 15-25 V). The Krebs solution in the organ bath was replaced by fresh, aerated Krebs solution at 37°C for each cycle. The tissue was deemed equilibrated once it reached a stable maximal isometric force (F_{max}) and a stable low resting tension. No strip with resting tension higher than 2% F_{max} was used for this study. To prevent active tone from developing, indomethacin was included in Krebs solution for all experiments [5 x 10^{-5} M].

3.2.2   Overview of experimental design

Ramp stretches were applied to muscle strips under various conditions and the force response measured. Fig. 3.1A shows raw data from a typical experiment. The ramp stretches were done in triplets (three identical stretches), where the rise of the stretch was 3 times the duration of the release back to L_{ref}. By changing the duration n (Fig. 3.1A) the amplitude and frequency of the ramp stretches could be altered. For sufficiently large amplitude of ramp stretches a biphasic force response could be seen during the first (and only the first) stretch. The initial phase (phase-1) of the force response is characterized by a relatively steep and almost linear rise in force. The later phase (phase-2) was identified as the force response after the transition point (Fig. 3.1B) which was characterized by a slower rise in force (Fig. 3.1B) in fully activated muscle. For partially activated muscle and for muscle in the presence of enzyme inhibitors that reduced force, the phase-2 was characterized by non-linear rise (sometimes a transient decrease) in force. Changes in the phase-1 and phase-2 responses were measured at different times after stimulation with maximal and sub-maximal doses of acetylcholine (10^{-7}-10^{-4} M ACh). The responses were also measured in the presence and absence of myosin light chain

kinase (MLCK) inhibitor ML-7, protein kinase C (PKC) inhibitor GF109203x, and Rho-kinase inhibitor H1152.

As a control observation to determine whether the ramp stretches caused any permanent decrease in the muscle's ability to generate force, we monitored force recovery after stretches with different amplitudes from 5-25% L_{ref}. With 5% stretches, the initial decrease in active force was ~15% and it recovered to the pre-stretch value in ~1 min. With a 10% stretch, the initial decrease in active force was ~35% and it recovered to the pre-stretch value in ~2 min. With a 25% stretch, the decrease in active force was ~85% and it recovered to the pre-stretch value in ~13 min. It was concluded that the experimental protocol would not lead to tissue damage.
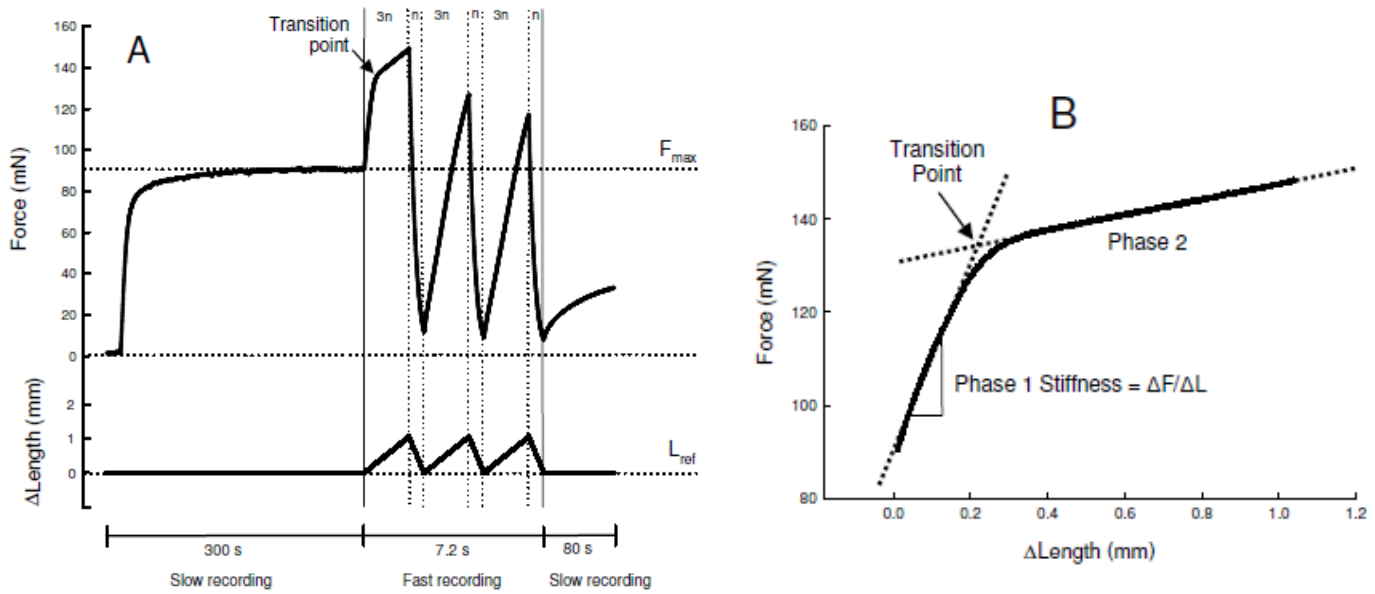
Figure 3.1 Method for ramp stretch and extrapolation of first stretch. A) Raw data showing force response to ramp stretches. The slow recording (20 samples/s) of the force and length data was interrupted by a fast recording (200 samples/s) to show the details during the ramp stretches. **B**) Force response during the first ramp stretch from panel A was plotted as a function of length change. The dotted line represents the average slope of the phase-1 response recorded during 0.1-0.3 s after the onset of the first stretch, and is defined as the phase-1 stiffness. The L_{ref} of the muscle was 7 mm, and the cross-sectional area of the muscle was 0.45 mm^2.

3.2.3 Measurement of phase-1 stiffness

In one group of experiments, the phase-1 stiffness was measured at different time points during a maximal contraction. The time points were 90, 150, 300, 600, and 900 s after stimulation with 10^{-4} M ACh. The triplets of ramp stretches were applied once per contraction as illustrated in Fig. 3.1A. The muscle was allowed to relax and rest for 15 min before induction of the next contraction and application of ramp stretches. The order of measurements at different time points was randomized. The phase-1 stiffness of the first stretch was defined as the average slope of the length-force plot (dotted line, Fig. 3.1B) between 0.1-0.3 s after the onset of the ramp stretch. The definition applied only to the condition where the rate of the iso-velocity stretch was 15% L_{ref} per 1.8 s. At this particular rate of stretch the time of transition between the two phases occurred at between 0.4-0.6 s after the onset of the ramp stretch. (Note that the transition time changes with different rates of stretch). In another group of experiments the phase-1 stiffness was measured in sub-maximally activated muscle at 600 s after stimulation with different concentrations of ACh.

The phase-1 stiffness measurement was corrected for the compliance of the muscle lever system. The force-extension relationship of the lever system (including the silk thread connecting the muscle preparation to the lever) was determined in the absence of the muscle preparation. The force-extension characteristics of the lever system were obtained so that the compliance of the system over the entire force range used in the experiments of this study could be determined. The compliance of the system was subtracted from the overall strain applied to the muscle in the calculation of the phase-1 stiffness.

3.2.4 Force response to ramp stretch in the presence and absence of inhibitors

Three inhibitors were used in this study to probe the signalling pathways governing the force responses. The concentration for each inhibitor was chosen so that the maximal force produced by the muscle (activated by 10^{-4} M ACh) in the presence of the inhibitor was reduced by 30-50% compared with that in the absence of inhibitor. A control was created by reducing [ACh] so that, in the absence of the inhibitor, the muscle produced the same amount of isometric

force as the muscle did in the presence of the inhibitor. The force-matched control and fully-activated control were both used in the comparison of ramp-stretch induced force responses with those produced in the presence of inhibitors.

The inhibitors used were H1152 (Rho-kinase inhibitor) from Torcris Bioscience, GF109203x (PKC inhibitor) from Enzo Biochem, and ML-7 (MLCK inhibitor) from Sigma-Aldrich. After equilibration of the tissue, F_{max} for the tissue was obtained with 10^{-4} M ACh; this provided a reference value for calculating the percent decrease in force due to interruption of the signalling pathways by each inhibitor. To achieve the target reduction in F_{max} (i.e., 30-50% reduction in isometric force) protocols for each inhibitor varied. For H1152, the muscle strips were incubated for 30 min at 3 μM of the inhibitor concentration; for GF109203x, the muscle strips were incubated for 50 min at 10 μM of the inhibitor concentration, and for ML-7, the muscle strips were incubated for 60 min at 20 μM of inhibitor concentration. For the group of experiments examining the effects of the inhibitors, the ramp stretches were applied at a fixed time, i.e., 600 s after the muscles were activated.

3.2.5   Statistics

For comparison of means, paired t-test and one-way ANOVA with repeated measures with Tukey post test analysis, and two-way ANOVA were used. Data are presented as means±SE, n indicates the number of tracheal muscle preparations from different sheep. SigmaPlot 11 and Prism Graphpad were used for statistical analyses.

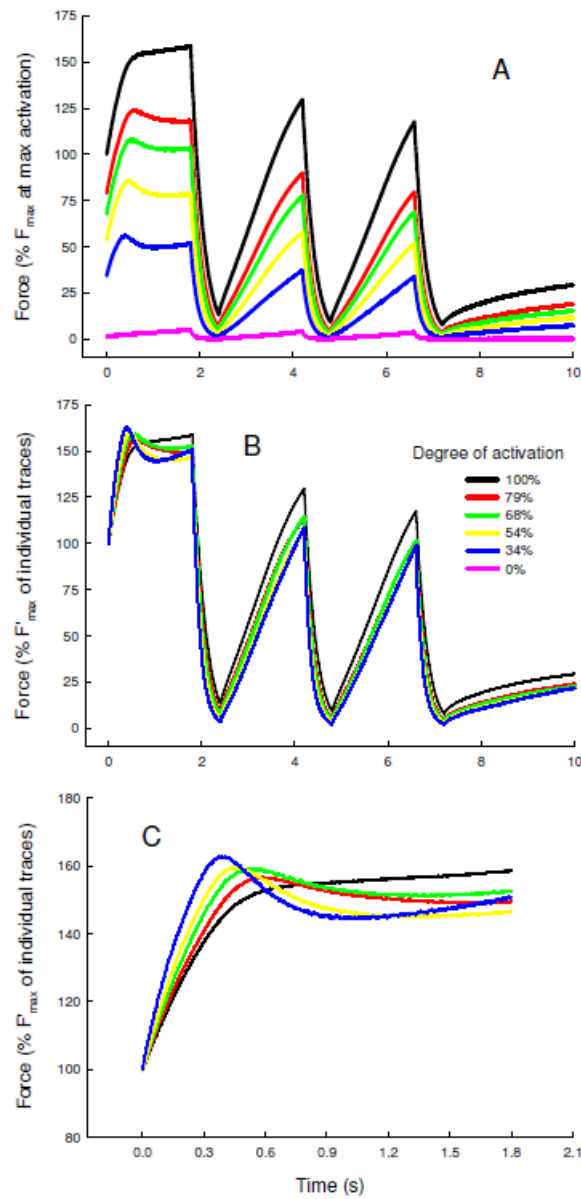### 3.3   Results

3.3.1   Force response to ramp stretch at different degrees of muscle activation

Fig. 3.2 shows force response to ramp stretches at different degrees of activation using different concentrations of ACh. In Fig. 3.2A all force values were normalized by the maximal isometric force (F_{max}) at which the first stretch was initiated. The percent activation was

represented by the plateau forces of individual traces as a percentage of the F_{max} of the maximally activated control (black trace). In Fig. 3.2B the force values were normalized by the values of maximal isometric force of the individual traces (F'_{max}). Note that F_{max} is used to represent maximal isometric force produced by maximally activated muscle, whereas F'_{max} is used to represent maximal isometric force produced at varying degrees of activation or by enzyme inhibited muscles. Because the same ramp stretches were applied to the muscle (Fig. 3.2B), the magnitude of the force response was directly proportional to the relative stiffness of the muscle. Here the relative stiffness was defined as the stiffness ($\Delta F/\Delta L$) divided by the value of F'_{max} at which the stiffness was measured. Fig. 3.2C (the same traces from Fig. 3.2B plotted at an expanded time scale) shows a decrease in phase-1 relative stiffness as the degree of activation was increased. However, the force response during the second and third stretch (Fig. 3.2B) showed an increase in relative stiffness as the degree of activation was increased.

The phase-2 response during the first stretch was highly non-linear, showing a reversal of slope (negative slope) in partially activated muscles (Fig. 3.2). The negative slope increased as the degree of activation was decreased.

Figure 3.2 Force response to ramp stretches at different degrees of activation induced by different concentrations of ACh. **A**) Force normalized to F_{max} of maximally (100%) activated muscle (10^{-4} M ACh, black solid line). Response from unstimulated resting muscle (pink line) was labeled as 0%. Each trace was an average of 4 traces of raw data. **B**) Same traces as in panel A but normalized to F'_{max}, the maximal isometric force of individual traces obtained at different degrees of activation. **C**) Same traces as in panel B but only the responses to the first ramp stretch were plotted. The 0% activation trace was not included in B and C.

Fig. 3.3A shows quantitative measurements of muscle stiffness ($\Delta F/\Delta L$ normalized by F_{max}) as a function of the degree of activation. A positive correlation ($r^2 = .9695$) was obtained. Fig. 3.3B shows relative stiffness ($\Delta F/\Delta L$ normalized by F'_{max}) as a function of the degree of activation. A negative correlation ($r^2 = 9778$) was obtained.
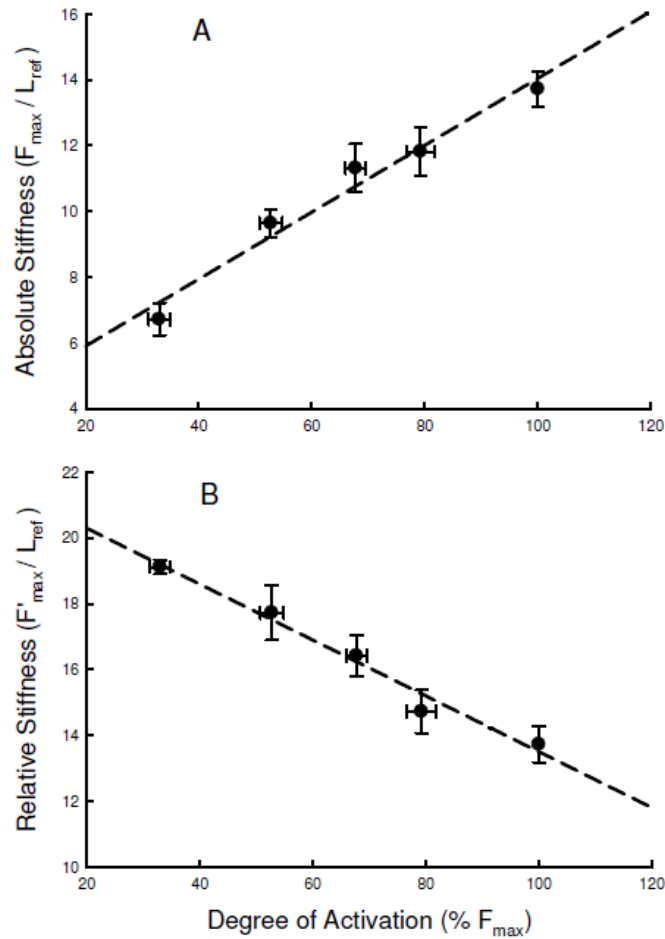
Figure 3.3 Normalizations of phase-1 stiffness at different degrees of activation. A) Phase-1 stiffness of muscle at different degrees of activation normalized by the maximal isometric force of maximally activated muscle (F_{max}). The dashed line is a linear fit to the data, with $r^2 = 0.9695$ and a significant positive slope of 0.102 ± 0.010 [$F_{max}/(L_{ref} \cdot \%F_{max})$] ($p < 0.05$). **B**) Phase-1 stiffness of muscle at different degrees of activation normalized by the plateau isometric force at the corresponding degree of activation (F'_{max}). The dashed line is a linear fit to the data, with $r^2 = 0.9778$ and a significant negative slope of -0.085 ± 0.008 [$F'_{max}/(L_{ref} \cdot \%F_{max})$].

3.3.2 Strain at transition point in maximally activated muscles

In maximally activated tracheal smooth muscle (10^{-4} M ACh) the transition point between phase-1 and phase-2 force response to ramp stretch could be determined by the cross point of the straight lines representing the average slopes of the two phases, as illustrated in Fig. 3.1B. The strain at which the transition point occurred under different conditions (different rates and amplitudes of stretches) was remarkably constant at slightly over 3% of L_{ref}, as shown in Fig. 3.4.
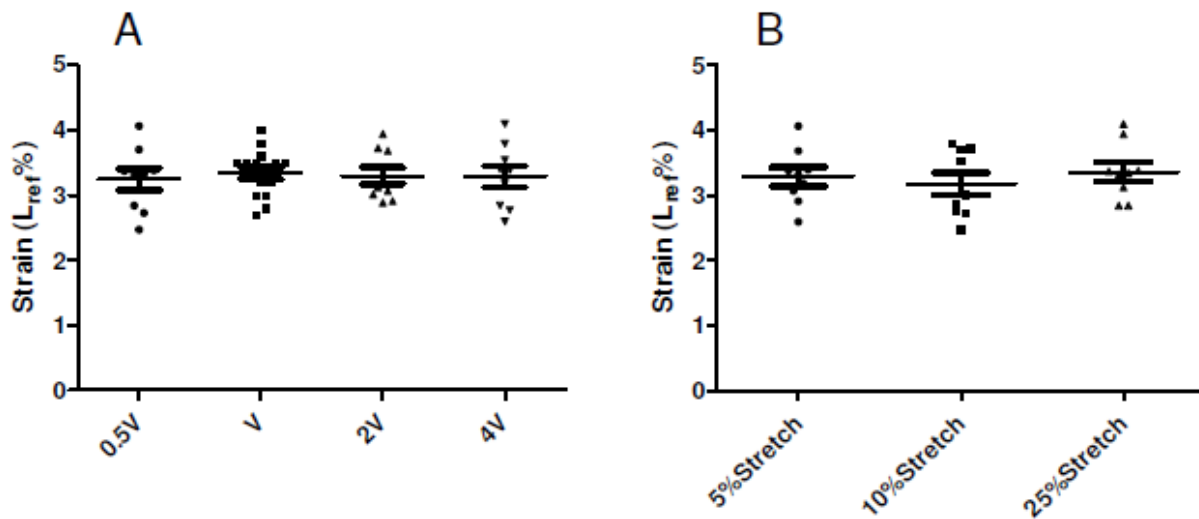
Figure 3.4: **Strain at transition point** measured under different speeds (A) and amplitudes (B) of ramp stretches applied at the plateau of maximal contractions (10^{-4} M ACh). The transition point was determined as illustrated in Fig. 3.1B. Note that this method applies only to maximal contractions where there is no negative slope in the phase-2 response. The reference velocity of stretch (V) was 25% L_{ref}/3s, approximately the rate of stretch during a deep inspiration. The reference velocity was used to obtain the data shown in panel B with different stretch amplitudes; %Stretch refers to percent of L_{ref}.

3.3.3 Phase-1 stiffness during the first and second stretch

In maximally activated tracheal smooth muscle, stiffness measured during the initial phase of the first and second stretches (illustrated in Fig. 3.5A) was measured with small amplitude (2% L_{ref}) of ramp stretches. At this amplitude of stretch, stiffness measured during the first stretch was not different from that measured during the second stretch (Fig. 3.5C). However, with large amplitude of stretch (15% L_{ref}) (Fig. 3.5B), stiffness measured during the second stretch was significantly less than that of the first stretch (Fig. 3.5D).
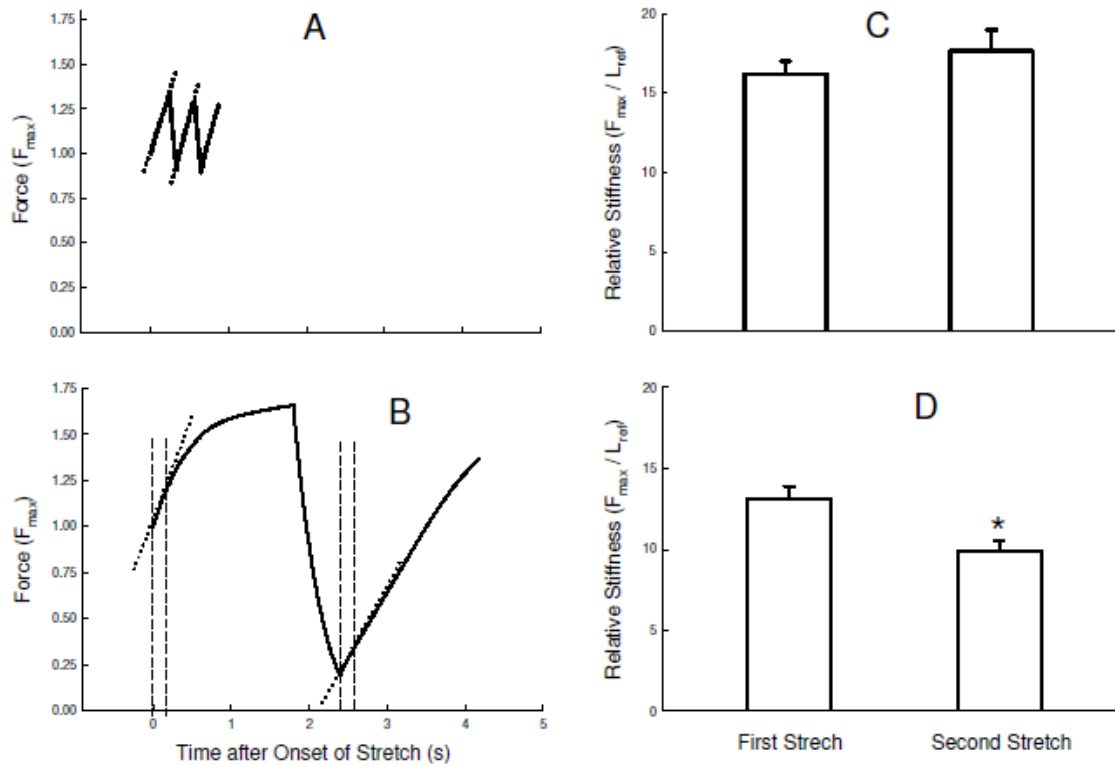
Figure 3.5 Comparison of values of stiffness obtained during the first and second stretches at different stretch amplitudes. With small (2% L_{ref}) amplitude of stretches the muscle stiffness (indicated by the slope of the dotted line) was not changed between the first and second stretch (**A**). With large (15% L_{ref}) amplitude of stretches the muscle stiffness was reduced in the second stretch (**B**). Note that because iso-velocity stretches were used during the measurement, length change is linearly proportional to time change, therefore changes in the slopes of the dotted lines in A and B can be used to indicate changes in stiffness. The changes in relative stiffness (normalized to F_{max}) were calculated from n=4 experiments and plotted in **C** and **D**. No difference in stiffness of first vs. second stretch was found with small stretches (C), whereas significant difference (p=0.014, paired t-test) in stiffness was found with large stretches (D).

3.3.4 Phase-1 stiffness at different time points on the plateau of maximal isometric contraction

Fig. 3.6A shows relative stiffness of tracheal smooth muscle measured at different times after stimulation with ACh (10^{-4} M). The data indicate that there is a time dependent increase in relative stiffness. The data also indicate that the stiffness increase is independent of isometric stress (Fig. 3.6B), which is different from the phenomenon of activation-dependent stiffness change observed in Fig. 3.3.
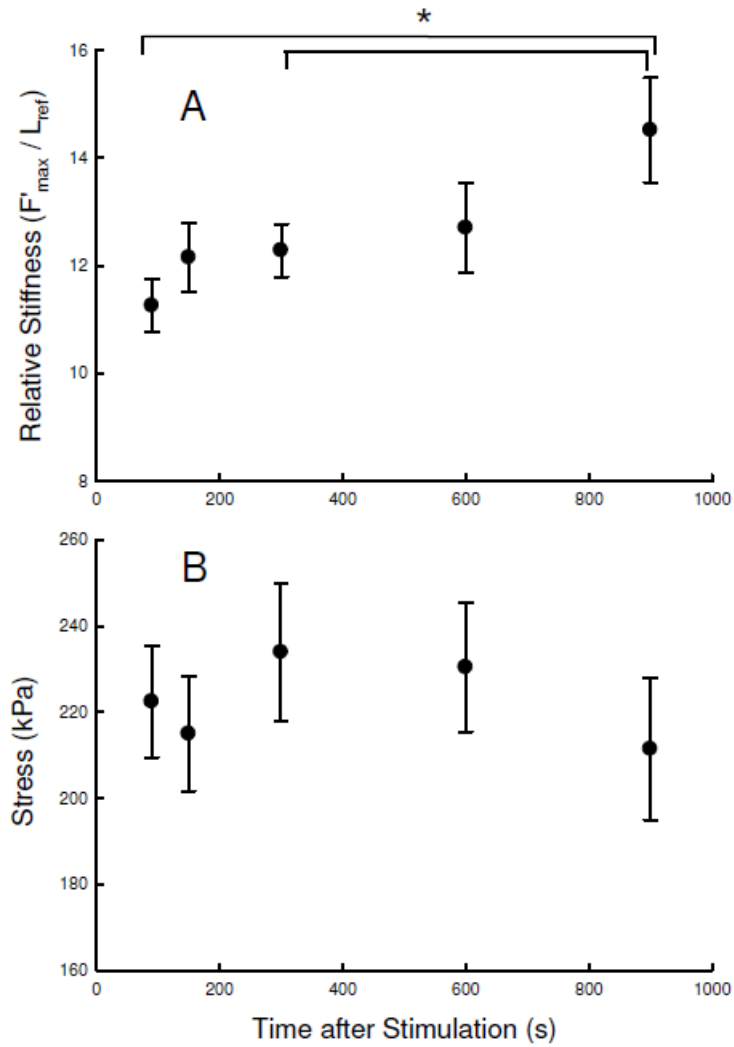
Figure 3.6 Phase-1 stiffness at different time points of contraction. (**A**) Stiffness of muscle at different times after stimulation normalized by the maximal isometric stress (**B**) at the time of first stretch. One-way ANOVA indicates that the stiffness increase with time is significant ($p<0.001$). Significant differences in stiffness were also found with multiple comparisons using Tukey test (indicated by *). Variation in isometric stress at different times after stimulation (shown in panel B) was not statistically different (One-way ANOVA, $p=0.219$).

3.3.5 Alteration in force response to ramp stretch in the presence and absence of enzyme inhibitors

Inhibitors of MLCK, PKC and Rho-kinase altered the force response to a ramp stretch. As shown in Fig. 3.7, each inhibitor has its own "signature" in the pattern of force response, possibly due to differential effects on the cross-bridge and cytoskeletal stiffness. Comparison of partial activation (gray curve) with full activation (black solid curve) in the absence of inhibitors (Fig.3.7) revealed that partial activation did not merely reduce the force response; it also altered the pattern of response. That is, the partial response is not an exact scaled down version of the full response. Inhibition of MLCK and PKC produced a pattern similar to that produced by partial activation (Fig. 3.7A and 3.7B). However, inhibition of Rho-kinase (Fig. 3.7B) produced a pattern different from that of partial activation.
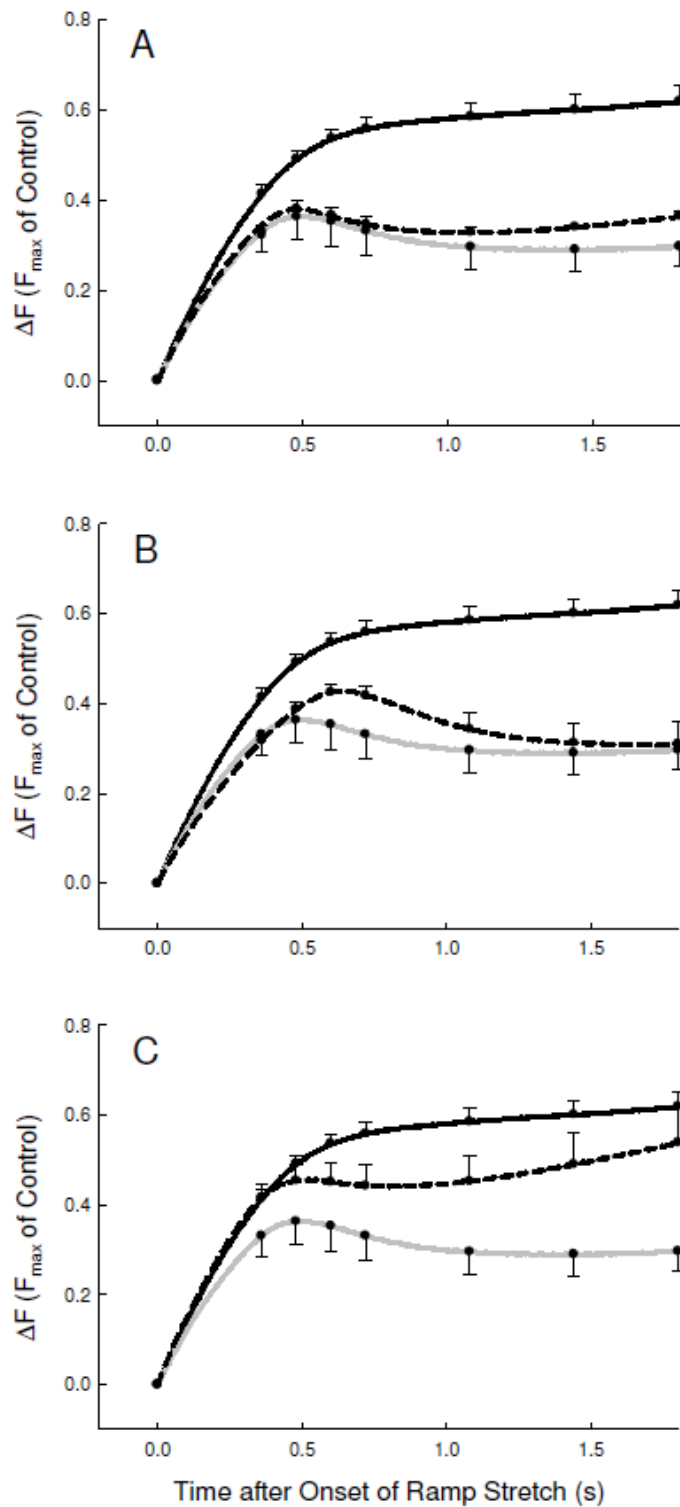
Figure 3.7 Comparison of force response to ramp stretch in the presence and absence of inhibitors (n=4). In each of the panels, the black solid curve is the fully activated control; the gray curve is the partially activated (force-matched) control; and the dashed curve is the test (i.e., fully activated with MLCK, PKC, or Rho-kinase inhibitor). **A**) Comparison of the fully and partially activated controls with force response in the presence of MLCK inhibitor ML-7. The

fully activated control is different from both the partially activated control and the ML-7 test (p<0.001); the ML-7 test is not different from the partially activated control (p=0.734). **B**) Comparison of the fully and partially activated controls with force response in the presence of PKC inhibitor GF109203x. The fully activated control is different from both the partially activated control and the GF109203x test (p<0.001); the GF109203x test is not different from the partially activated control (p=0.617). **C**) Comparison of the fully and partially activated controls with force response in the presence of Rho-kinase inhibitor H1152. The fully activated control is different from the partially activated control (p<0.001) but not different from the H1152 test (p=0.086); the Rho-kinase test is different from the partially activated control (p=0.003).

Fig. 3.8 shows quantitative phase-1 stiffness data that were shown in Fig. 3.7 graphically. Inhibition of MLCK and PKC produced similar changes in phase-1 stiffness as partial activation did compared to that observed in full activation (Fig. 3.8). Inhibition of Rho-kinase, however, did not reduce the phase-1 stiffness (Fig. 3.8).
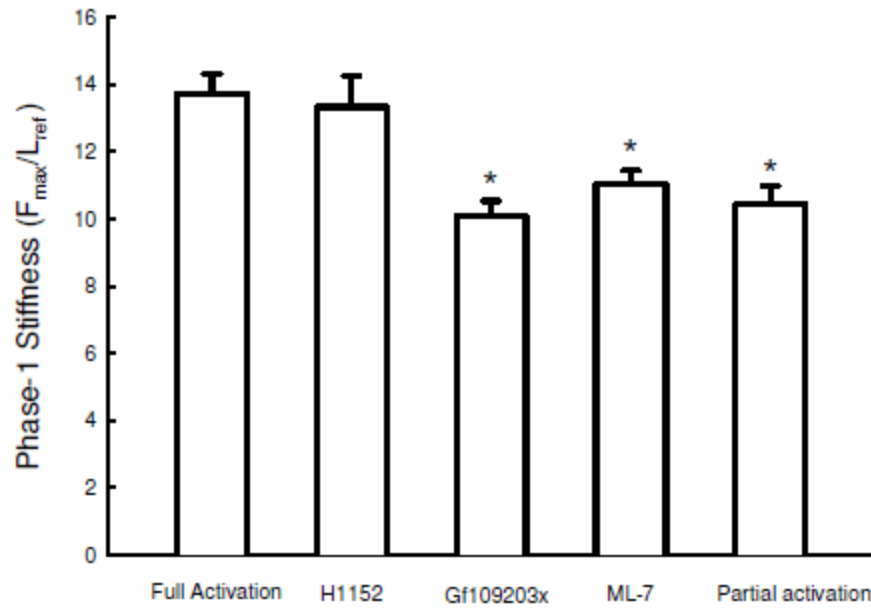
Figure 3.8 Phase-1 stiffness under different inhibitor conditions. Both full and partial activation controls were obtained without inhibitors. The tests were obtained in fully activated muscles incubated with inhibitors labeled on the graph. *, significantly different from the fully activated control ($p<0.05$).

3.4   Discussion

Force response to cycles of ramp stretch and release in airway smooth muscle offers an opportunity to examine the mechanisms underlying the ability of the muscle to generate and maintain force in a mechanically dynamic environment. The characteristic biphasic force response allows us to dissect out components in the muscle responsible for each of the phases of the response and facilitates identification of candidate structural proteins and their regulation by enzymes in modulating muscle properties for optimal function in the airways.

3.4.1   Actomyosin interaction is largely responsible for the phase-1 response

As in striated muscle, the initial phase of the force response to ramp stretch likely stems mainly from the attached myosin crossbridges (Edman 1999; Getz, Cooke, and Lehman 1998; Lombardi and Piazzesi 1990; Pinniger, Ranatunga, and Offer 2006). This is supported by several lines of evidence revealed by the present study. Firstly, in the relaxed muscle there was minimal response to the ramp stretches (Fig. 3.2A, pink trace); significant response was observed only in activated muscle. Secondly, the absolute phase-1 stiffness was found to be linearly correlated with the degree of activation (Fig. 3.3A). Similar phenomena have been observed (24, 26), and the common explanation is that the number of attached crossbridges increases with the degree of muscle activation. Thirdly, the relative phase-1 stiffness was found to be negatively correlated with the degree of activation (Fig. 3.3B). This is also a well-known crossbridge related phenomenon. In partially activated muscle it has been shown that the stiffness is disproportionally higher relative to force (Martyn and Gordon 1992), and this can be explained by a model for muscle stiffness that considers both the crossbridge and myofilament compliance (Mijailovich, Fredberg, and Butler 1996). Another explanation based on known cross-bridge properties is that a greater proportion of the cross-bridges in partially activated muscle are in the low-force state (i.e., attached but not yet through the power-stroke). This would also lead to disproportionally higher stiffness relative to force (C. Y. Seow and Ford 1993). As discussed later in more detail, a minor component of the phase-1 stiffness could stem from the cytoskeleton (which could contribute to the increase in the relative stiffness with lower levels of activation) if we assume that stiffening of the cytoskeleton is more sensitive (compared with cross-bridge

stiffness) to the level of muscle activation. However, based on the large change in the absolute and relative stiffness with respect to the degree of activation observed in the present study (Fig. 3.3) it is likely that the phase-1 response originates mainly from stretching the myofilament lattice with attached crossbridges. Another line of evidence comes from the observation that a "break" point (i.e., the transition point between phase-1 and phase-2, see Fig. 3.1B) occurs during a large amplitude stretch, and that it occurs at the same strain (about 3.3% L_{ref}) regardless of the speed and amplitude of stretch, as long as the amplitude is greater than the strain at the breakpoint (Fig. 3.4). This suggests that the phase-1 response stems from some structure that yields after a certain amount of strain. This structure is likely the crossbridges. It is known that the average range of motion of an attached bridge in striated muscle is about 13 nm (Ford, Huxley, and Simmons 1977). This is about 1.2% of the half-sarcomere length. If the average range of motion of attached bridges in smooth muscle is the same as that of striated muscle, the attached crossbridges on either side of a side-polar myosin filament of smooth muscle would have about 2.4% of motion range. This is within the range of 3.3% shown in Fig. 3.4. Because the smooth muscle preparations we used consisted of bundles of cells in parallel and in series, the compliance in the cell-to-cell connection and other intra- and extracellular structures in series with the contractile units could easily make up the difference between 2.4% and 3.3%. In comparison of experimental data with a theoretical model of actomyosin cross-bridge interaction, Mijailovich et al (Mijailovich, Butler, and Fredberg 2000) have shown that the model prediction of hysteresivity (a measure of how closely a change in force follows a change in length) deviates significantly from data when the amplitude of length oscillation exceeds a value between 2-4%, indicating that when a critical strain (similar to what we found in the present study) is surpassed the cross-bridge model no longer simulates real muscle behavior, because the model does not take cytoskeletal remodelling into account.

Although the phase-1 stiffness likely stems mainly from the cross-bridges, a minor contribution to the breakpoint strain from the cytoskeleton (such as cross-linkers connecting cytoskeletal filaments) cannot be excluded. The constant strain at which the muscle yielded (Fig. 3.4) can be taken as evidence that the phase-1 response is mostly crossbridge related and that the stiffness mostly reflects the stiffness related to attached cross-bridges and to a lesser extent, the cross-linkers. Unfortunately the motion range for attached cross-linkers is currently unknown.

3.4.2 The effects of partial activation on phase-2 and subsequent responses

From Fig. 3.2C it is clear that the negative slope in the phase-2 response increases with decreasing degree of activation. If the phase-2 response is due to reattachment of forcibly detached crossbridges during the stretch (Getz, Cooke, and Lehman 1998; Lombardi and Piazzesi 1990), the results indicate that the rate of reattachment is dependent on the degree of activation in smooth muscle. That is, the rate decreases with decreasing degree of activation. This reduced rate of reattachment also explains the lower amplitude of relative force response in partially activated muscle seen in the second and third stretches, even though during the first stretch the opposite was true (Fig. 3.2B). Note that prior to the first stretch the crossbridges have sufficient time for attachment to actin filaments and the rate of attachment plays no role in determining the amplitude of the force response during the first stretch.

It is interesting to note that the point of force inflection during the first stretch in partially activated muscles occurs at earlier times (Fig. 3.2C). This indicates that the crossbridges on average detach at a smaller strain in partially activated muscle compared to that in fully activated muscle. In maximally activated muscle the strain at which the force inflection (breakpoint) occurs has been shown to be independent of speed and amplitude of stretch (Fig. 3.4). One explanation for why the breakpoint strain in partially activated muscle is smaller than that in fully activated muscle is that in fully activated muscle a greater fraction of the crossbridges are in the post power-stroke state of the crossbridge cycle. The motion range of a post power-stroke bridge is greater than that of a pre power-stroke bridge because for a post power-stroke crossbridge to detach it has to undergo a reversal of power stroke first (which puts the post power stroke bridge in the same conformation as a pre power stroke bridge) before it detaches. In addition, it is possible that the post power-stroke bridges have a greater binding force to actin filaments compared to the pre power-stroke bridges, and therefore can withstand a larger strain before detachment.

3.4.3   Time dependence of phase-1 stiffness

As shown in Fig. 3.6A, the relative phase-1 stiffness of airway smooth muscle increases with time during which isometric plateau force is maintained. This change in stiffness is not related to variations in the degree of activation (as it is in the case shown in Fig. 3.3B), because the maximal isometric force (F_{max}) during the time examined did not change (Fig. 3.6B). The results suggest that in a sustained contraction stiffening of the cytoskeleton occurs. This explanation is based on the assumption that stiffening of the cytoskeleton (possibly by formation of cross-linkers that stabilize the cytoskeletal filament network) does not contribute to force generation (as crossbridges do) and therefore results in a disproportional increase in stiffness over force, i.e., an increase in relative stiffness.

3.4.4   Modulation of the force response by enzyme inhibitors

In the present study we chose to examine the consequence of partially inhibiting three enzymes known to be part of the signalling pathways regulating smooth muscle contraction. The inhibitors of MLCK, PKC, and Rho-kinase interrupt different pathways (Puetz, Lubomirov, and Pfitzer 2009). Inhibition by different enzymes produced quantifiable differences in the force response to ramp stretch. Overall all interventions produced about a 30-50% decrease in isometric force (from the fully activated control); the changes in force in response to ramp stretches are compared in Fig. 3.7.

Inhibition of MLCK in airway smooth muscle is known to reduce the degree of phosphorylation of the regulatory myosin light chain and active force (Qi et al. 2002). Not surprisingly the effect of MLCK inhibition on the force response to ramp stretch is similar to that of partial activation that produced the same degree of force reduction as MLCK inhibition (Fig. 3.7A). A likely explanation is that MLCK inhibition reduces the number of attached crossbridges and also reduces the rate of crossbridge reattachment during the phase-2 response.

Inhibition of PKC also had a similar effect on the force response as did partial activation (Fig. 3.7B). PKC is known to phosphorylate (activate) the phosphopeptide CPI-17, which is an

inhibitor of the myosin light chain phosphatase (MLCP) once activated. Phosphorylation of the myosin phosphatase subunit1 (MYPT1) by PKC is also known to reduce MLCP activity (Puetz, Lubomirov, and Pfitzer 2009). Inhibition of PKC therefore will increase MLCP activity and reduce the level of MLC phosphorylation. This could explain why PKC and MLCK inhibition resulted in similar changes in force response (Fig. 3.7A & B) and suggests that at least in airway smooth muscle the main effect of PKC and MLCK inhibition is in reducing the number of activated cross-bridges (as evidenced by the reduced phase-1 stiffness in Fig. 3.8) and the rate of cross-bridge reattachment to actin filaments (as evidenced by the negative slope in phase-2 in Fig. 3.7A & B).

Inhibition of Rho-kinase did not produce a significant change in the force response (Fig. 3.7C). Notably phase-1 stiffness was not altered by Rho-kinase inhibition (Fig. 3 8), despite a 50% decrease in isometric force. This suggests that Rho-kinase inhibition did not alter the number of attached bridges, but reduced force produced per bridge, possibly by slowing the transition between low-force and high-force states (the power stroke). This may limit the muscle's ability to maintain force during prolonged contraction under continuous length oscillation. This is consistent with the results of Lan et al (Lan et al. 2015) who showed that inhibition of Rho-kinase in airway smooth muscle leads to a more rapid and greater extent of force decline during a prolonged contraction. Rho-kinase also regulates many pathways that modify the mechanical properties of cytoskeleton (Puetz, Lubomirov, and Pfitzer 2009) such as through actin polymerization and filament anchoring. However, these activities and their regulation by Rho-kinase are likely too complex to be discerned by at the molecular level by just examining the force response to a ramp stretch.

3.4.5 Relevance to airway and lung function

The observation that exceeding a critical strain (~3.3% L_{ref}, Fig. 3.4) during a ramp stretch is needed to significantly reduce the stiffness of airway smooth muscle implies that a deep inspiration is effective in bronchodilation (Skloot, Permutt, and Togias 1995) only when the critical strain in airway smooth muscle is exceeded in vivo. As shown in Fig. 3.5A and 5C, an oscillation with 2% L_{ref} amplitude was not sufficient to cause a decrease in phase-1 stiffness in

airway smooth muscle. In Fig. 3.5B and 5D, an oscillation with 15% L_{ref} amplitude is shown to cause a decrease in phase-1 stiffness after the first stretch. (This has also been shown for 5% and 10% L_{ref} amplitude oscillations, data not shown). Measurements of bronchial muscle strain and bronchodilation by Ansell et al in isolated bronchial segments showed evidence for the existence of such a critical strain (Ansell et al. 2014). Their data showed that strains less than ~3% are ineffective in causing any bronchodilation and that bronchodilation is observed only when strain amplitude is greater than ~3%. The abrupt change in strain-dependent bronchodilation shown by Ansell et al at a strain value very similar to that found in airway smooth muscle strips (Fig. 3.4) suggests that the mechanism underlying bronchodilation in airway segments is related to the biphasic behavior of airway smooth muscle subjected to stretch. Once the crossbridge attachment is broken, the reduced airway stiffness likely renders bronchial smooth muscle more susceptible to strain softening which may involve further breaking of non-crossbridge cytoskeletal linkers, leading to a sustained state of bronchodilation (fluidization) as long as the oscillatory strain is maintained (4).

Results presented in Fig. 3.6 suggest that prolonged contraction of airway smooth muscle could lead to a "frozen" state as described by Gunst and Fredberg (Susan J. Gunst and Fredberg 2003), with the muscle stiffness increasing with time. As postulated by Gunst and Fredberg, during the time course of isometric contraction the cytoskeletal lattice stabilizes, solidifies, and forms a rigid structure for transmission of force generated by the actomyosin interaction. The increase in phase-1 relative stiffness is consistent with this line of interpretation, because unlike absolute stiffness, relative stiffness signifies an increase in stiffness without a concomitant increase in force, indicating that the stiffness increase is related to changes in non-force generating elements, i.e., solidification of the cytoskeleton.

The phase-2 force response to a ramp stretch likely stems from multiple components of the muscle machinery. In skeletal muscle the rate of cross-bridge reattachment after detachment is the most important factor determining the shape of the phase-2 response. It is likely that the same mechanism underlies at least part of the smooth muscle response. Changes in the slope of the phase-2 response under different conditions therefore could be used as an approximate measure of the effect of different experimental interventions on the rate of cross-bridge

reattachment. However, it is important that the role of cytoskeleton in determining the phase-2 response be considered in any analysis. In examining the response of airway smooth muscle to oscillatory strains, Oliver et al have shown that at low frequencies and high strain amplitudes there are discrepancies between predictions from a crossbridge model and data from experiments. They have concluded that "These discrepancies thus expose a new domain of slow dynamics that cannot be accounted for by actomyosin interactions. Rather, we suggest that these slow dynamics are attributable to cytoskeletal remodelling (microstructural rearrangement) that is ongoing during slow deformations" (Oliver et al. 2010). Although our experimental approach is different from theirs, a similar conclusion can be made from the results of the present study.

The fact that there are two phases in the response to strain in airway smooth muscle has potential physiological and clinical significance. There is increasing evidence that differential responsiveness to the strains induced by breathing maneuvers contributes to airway hyperresponsiveness (An et al. 2007; Skloot, Permutt, and Togias 1995). The bronchodilatory response to strain is altered during an acute attack of asthma, that is, it is reduced compared to that seen when a similar degree of airway obstruction is induced by an inhaled spasmogen (Lim et al. 1989). A recent study found that airway smooth muscle stiffness could be targeted to increase the efficacy of bronchodilatory drugs (Ansell et al. 2014). These observations suggest that pharmacological interventions designed to modulate the stiffness as well as the contractile responses of airway smooth muscle could have a complimentary or even synergistic beneficial effect.

3.5 Conclusion

ASM response to a ramp stretch showed a biphasic feature, with the initial phase associated with greater muscle stiffness compared with that in the later phase; and that the transition between the phases occurred at a critical strain of ~3.3%. Only strains with amplitudes greater than the critical strain could lead to reduction in force and stiffness of the muscle in the subsequent stretches. The initial phase stiffness was found to be linearly related to the degree of muscle activation, suggesting that the stiffness stems mainly from attached cross-bridges. Both

phases were affected by the degree of muscle activation, and by inhibitors of myosin light chain kinase, protein kinase C, and Rho-kinase. Different responses due to different interventions suggest that cross-bridge and cytoskeletal stiffness are regulated differently by the kinases.

Bibliography

Amano, M., M. Nakayama, and K. Kaibuchi. 2010. "Rho-kinase/ROCK: A Key Regulator of the Cytoskeleton and Cell Polarity." *Cytoskeleton (Hoboken, N.J.)* 67 (9): 545–54. doi:10.1002/cm.20472.

Ansell, T. K., P. B. Noble, H. W. Mitchell, and P. K. McFawn. 2014a. "Pharmacological Bronchodilation Is Partially Mediated by Reduced Airway Wall Stiffness." *British Journal of Pharmacology* 171 (19): 4376–84. doi:10.1111/bph.12781. 2014b. "Pharmacological Bronchodilation Is Partially Mediated by Reduced Airway Wall Stiffness." *British Journal of Pharmacology* 171 (19): 4376–84. doi:10.1111/bph.12781.

Bai, Tony R., J. H. T. Bates, V. Brusasco, B. Camoretti-Mercado, P. Chitano, L. Deng, M. Dowell, et al. 2004. "On the Terminology for Describing the Length-Force Relationship and Its Changes in Airway Smooth Muscle." *Journal of Applied Physiology (Bethesda, Md. : 1985)* 97 (6): 2029–34. doi:10.1152/japplphysiol.00884.2004.

Bosse, Y., L. Y. M. Chin, Peter D. Pare, and Chun Y. Seow. 2009. "Adaptation of Airway Smooth Muscle to Basal Tone: Relevance to Airway Hyperresponsiveness." *American Journal of Respiratory Cell and Molecular Biology* 40 (1): 13–18. doi:10.1165/rcmb.2008-0150OC.

Bosse, Y., L. Y. M. Chin, P. D. Pare, and C. Y. Seow. 2010. "Chronic Activation in Shortened Airway Smooth Muscle: A Synergistic Combination Underlying Airway Hyperresponsiveness?" *American Journal of Respiratory Cell and Molecular Biology* 42 (3): 341–48. doi:10.1165/rcmb.2008-0448OC.

Bosse, Y., A. Sobieszek, P. D. Pare, and C. Y. Seow. 2008. "Length Adaptation of Airway Smooth Muscle." *Proceedings of the American Thoracic Society* 5 (1): 62–67. doi:10.1513/pats.200705-056VS.

Brook, B. S. 2014. "Emergence of Airway Smooth Muscle Mechanical Behavior through Dynamic Reorganization of Contractile Units and Force Transmission Pathways." *Journal of Applied Physiology (Bethesda, Md. : 1985)* 116 (8): 980–97. doi:10.1152/japplphysiol.01209.2013.

Brown, R.H., and W. Mitzner. 2003. "Airway Response to Deep Inspiration: Role of Nitric Oxide." *European Respiratory Journal* 22 (1): 57–61. doi:10.1183/09031936.03.00090403.

Brown, R. H., N. Scichilone, B. Mudge, F. B. Diemer, S. Permutt, and A. Togias. 2001. "High-Resolution Computed Tomographic Evaluation of Airway Distensibility and the Effects of Lung Inflation on Airway Caliber in Healthy Subjects and Individuals with Asthma." *American Journal of Respiratory and Critical Care Medicine* 163 (4). doi:10.1164/ajrccm.163.4.2007119.

Bursac, P., G. Lenormand, B. Fabry, M. Oliver, D. A. Weitz, V. Viasnoff, J. P. Butler, and J. J. Fredberg. 2005. "Cytoskeletal Remodelling and Slow Dynamics in the Living Cell." *Nature Materials* 4 (7): 557–61. doi:10.1038/nmat1404.

Cazzola, M., C. P. Page, L. Calzetta, and M. Gabriella Matera. 2012. "Pharmacology and Therapeutics of Bronchodilators." *Pharmacological Reviews* 64 (3). doi:10.1124/pr.111.004580.

Chapman, D. G., G. G. King, N. Berend, C. Diba, and C. M. Salome. 2010. "Avoiding Deep Inspirations Increases the Maximal Response to Methacholine without Altering

Sensitivity in Non-Asthmatics." *Respiratory Physiology & Neurobiology* 173 (2): 157–63. doi:10.1016/j.resp.2010.07.011.

Chen, C., R. Krishnan, E. Zhou, A. Ramachandran, D. Tambe, K. Rajendran, R. M. Adam, L. Deng, and J. J. Fredberg. 2010a. "Fluidization and Resolidification of the Human Bladder Smooth Muscle Cell in Response to Transient Stretch." *PloS One* 5 (8). doi:10.1371/journal.pone.0012035.

Chin, L. Y. M., Y. Bosse, C. Pascoe, T. L. Hackett, C. Y. Seow, and P. D. Pare. 2012. "Mechanical Properties of Asthmatic Airway Smooth Muscle." *The European Respiratory Journal* 40 (1). doi:10.1183/09031936.00065411.

Colebatch, H. J., K. E. Finucane, and M. M. Smith. 1973. "Pulmonary Conductance and Elastic Recoil Relationships in Asthma and Emphysema." *Journal of Applied Physiology* 34 (2): 143–53.

Deng, L., X. Trepat, J. P. Butler, E. Millet, K. G. Morgan, D. A. Weitz, and J. J. Fredberg. 2006. "Fast and Slow Dynamics of the Cytoskeleton." *Nature Materials* 5 (8): 636–40. doi:10.1038/nmat1685.

Dillon, P. F., M.O. Aksoy, S. P. Driska, and R. A. Murphy. 1981. "Myosin Phosphorylation and the Cross-Bridge Cycle in Arterial Smooth Muscle." *Science* 211 (4481): 495–97. doi:10.1126/science.6893872.

Doeing, D. C., and J. Solway. 2013. "Airway Smooth Muscle in the Pathophysiology and Treatment of Asthma." *Journal of Applied Physiology (Bethesda, Md. : 1985)* 114 (7): 834–43. doi:10.1152/japplphysiol.00950.2012.

Donovan, G. M. 2013. "Modelling Airway Smooth Muscle Passive Length Adaptation via Thick Filament Length Distributions." *Journal of Theoretical Biology* 333 (September): 102–8. doi:10.1016/j.jtbi.2013.05.013.

Donovan, G. M., S. R. Bullimore, A. J. Elvin, M. H. Tawhai, J. H. T. Bates, A-M. Lauzon, and J. Sneyd. 2010. "A Continuous-Binding Cross-Linker Model for Passive Airway Smooth Muscle." *Biophysical Journal* 99 (10): 3164–71. doi:10.1016/j.bpj.2010.09.031.

Dowell, M. L., O. J. Lakser, W. T. Gerthoffer, J. J. Fredberg, G. L. Stelmack, A. J. Halayko, J. Solway, and R. W. Mitchell. 2005. "Latrunculin B Increases Force Fluctuation-Induced Relengthening of ACh-Contracted, Isotonically Shortened Canine Tracheal Smooth Muscle." *Journal of Applied Physiology (Bethesda, Md. : 1985)* 98 (2): 489–97. doi:10.1152/japplphysiol.01378.2003.

Edman, K. A. P. 1999. "The Force Bearing Capacity of Frog Muscle Fibres during Stretch: Its Relation to Sarcomere Length and Fibre Width." *The Journal of Physiology* 519 (Pt 2): 515–26. doi:10.1111/j.1469-7793.1999.0515m.x.

Ford, L. E., A. F. Huxley, and R. M. Simmons. 1977. "Tension Responses to Sudden Length Change in Stimulated Frog Muscle Fibres near Slack Length." *The Journal of Physiology* 269 (2).

Frearson, N., B.W.W. Focant, and S.V. Perry. 1976. "Phosphorylation of a Light Chain Component of Myosin from Smooth Muscle." *FEBS Letters* 63 (1): 27–32. doi:10.1016/0014-5793(76)80187-1.

Fredberg, J. J., D. S. Inouye, S. M. Mijailovich, and J. P. Butler. 1999. "Perturbed Equilibrium of Myosin Binding in Airway Smooth Muscle and Its Implications in Bronchospasm." *American Journal of Respiratory and Critical Care Medicine* 159 (3): 959–67. doi:10.1164/ajrccm.159.3.9804060.

Gamble, J., M. Stevenson, E. McClean, and L. G. Heaney. 2009. "The Prevalence of

Nonadherence in Difficult Asthma." *American Journal of Respiratory and Critical Care Medicine* 180 (9): 817–22. doi:10.1164/rccm.200902-0166OC.

Getz, E. B., R. Cooke, and S. L. Lehman. 1998. "Phase Transition in Force during Ramp Stretches of Skeletal Muscle." *Biophysical Journal* 75 (6): 2971–83. doi:10.1016/S0006-3495(98)77738-0.

Gunst, S. J. 1983. "Contractile Force of Canine Airway Smooth Muscle during Cyclical Length Changes." *Journal of Applied Physiology: Respiratory, Environmental and Exercise Physiology* 55 (3): 759–69.

Gunst, S. J., R. A. Meiss, M. F. Wu, and M. Rowe. 1995a. "Mechanisms for the Mechanical Plasticity of Tracheal Smooth Muscle." *The American Journal of Physiology* 268 (5 Pt 1): C1267–76.

Gunst, S. J., and J. J. Fredberg. 2003. "The First Three Minutes: Smooth Muscle Contraction, Cytoskeletal Events, and Soft Glasses." *Journal of Applied Physiology (Bethesda, Md. : 1985)* 95 (1): 413–25. doi:10.1152/japplphysiol.00277.2003.

Hai, C. M., and R. A. Murphy. 1988a. "Cross-Bridge Phosphorylation and Regulation of Latch State in Smooth Muscle." *The American Journal of Physiology* 254 (1 Pt 1). 1988b. "Cross-Bridge Phosphorylation and Regulation of Latch State in Smooth Muscle." *The American Journal of Physiology* 254 (1 Pt 1).

Harvey, B. C., Harikrishnan Parameswaran, and Kenneth R. Lutchen. 2013. "Can Tidal Breathing with Deep Inspirations of Intact Airways Create Sustained Bronchoprotection or Bronchodilation?" *Journal of Applied Physiology (Bethesda, Md. : 1985)* 115 (4): 436–45. doi:10.1152/japplphysiol.00009.2013.

Herrera, A. M., E. C. Martinez, and C. Y. Seow. 2004. "Electron Microscopic Study of Actin Polymerization in Airway Smooth Muscle." *American Journal of Physiology. Lung Cellular and Molecular Physiology* 286 (6): L1161–68. doi:10.1152/ajplung.00298.2003.

Hirshman, C. A., and C. W. Emala. 1999. "Actin Reorganization in Airway Smooth Muscle Cells Involves Gq and Gi-2 Activation of Rho." *The American Journal of Physiology* 277 (3 Pt 1): L653–61.

Hirshman, C. A., D. Zhu, T. Pertel, R. A. Panettieri, and C. W. Emala. 2005. "Isoproterenol Induces Actin Depolymerization in Human Airway Smooth Muscle Cells via Activation of an Src Kinase and GS." *American Journal of Physiology. Lung Cellular and Molecular Physiology* 288 (5): L924–31. doi:10.1152/ajplung.00463.2004.

Hirshman, C. A., H. Togashi, D. Shao, and C. W. Emala. 1998. "Galphai-2 Is Required for Carbachol-Induced Stress Fiber Formation in Human Airway Smooth Muscle Cells." *The American Journal of Physiology* 275 (5 Pt 1): L911–16.

Hirshman, C. A., D. Zhu, R. A. Panettieri, and C. W. Emala. 2001. "Actin Depolymerization via the Beta-Adrenoceptor in Airway Smooth Muscle Cells: A Novel PKA-Independent Pathway." *American Journal of Physiology. Cell Physiology* 281 (5): C1468–76.

Huang, Y., R. N. Day, and S. J. Gunst. 2014. "Vinculin Phosphorylation at Tyr1065 Regulates Vinculin Conformation and Tension Development in Airway Smooth Muscle Tissues." *The Journal of Biological Chemistry* 289 (6): 3677–88. doi:10.1074/jbc.M113.508077.

Huang, Y., W. Zhang, and S. J. Gunst. 2011. "Activation of Vinculin Induced by Cholinergic Stimulation Regulates Contraction of Tracheal Smooth Muscle Tissue." *The Journal of Biological Chemistry* 286 (5): 3630–44. doi:10.1074/jbc.M110.139923.

Huxley, A. F. 1957. "Muscle structure and theories of contraction." *Progress in biophysics and biophysical chemistry* 7.

Ishihara, H., H. Ozaki, K. Sato, M. Hori, H. Karaki, S. Watabe, Y. Kato, N. Fusetani, K. Hashimoto, and D. Uemura. 1989. "Calcium-Independent Activation of Contractile Apparatus in Smooth Muscle by Calyculin-A." *The Journal of Pharmacology and Experimental Therapeutics* 250 (1): 388–96.

Jones, K. A., W. J. Perkins, R. R. Lorenz, Y. S. Prakash, G. C. Sieck, and D. O. Warner. 1999. "F-Actin Stabilization Increases Tension Cost during Contraction of Permeabilized Airway Smooth Muscle in Dogs." *The Journal of Physiology* 519 Pt 2 (September): 527–38.

Kamm, K. E., and J. T. Stull. 1986. "Activation of Smooth Muscle Contraction: Relation between Myosin Phosphorylation and Stiffness." *Science (New York, N.Y.)* 232 (4746): 80–82.

Kapsali, T., S. Permutt, B. Laube, N. Scichilone, and A. Togias. 2000. "Potent Bronchoprotective Effect of Deep Inspiration and Its Absence in Asthma." *Journal of Applied Physiology (Bethesda, Md. : 1985)* 89 (2): 711–20.

Kim, H. R., M. Hoque, and C.-M. Hai. 2004. "Cholinergic Receptor-Mediated Differential Cytoskeletal Recruitment of Actin- and Integrin-Binding Proteins in Intact Airway Smooth Muscle." *American Journal of Physiology. Cell Physiology* 287 (5): C1375–83. doi:10.1152/ajpcell.00100.2004.

King, G. G., B. J. Moore, C. Y. Seow, and P. D. Pare. 1999. "Time Course of Increased Airway Narrowing Caused by Inhibition of Deep Inspiration during Methacholine Challenge." *American Journal of Respiratory and Critical Care Medicine* 160 (2): 454–57. doi:10.1164/ajrccm.160.2.9804012.

Kitazawa, T., and A. P. Somlyo. 1991. "Modulation of Ca2+ Sensitivity by Agonists in Smooth Muscle." *Advances in Experimental Medicine and Biology* 304.

Krishnan, R., C. Y. Park, Y.-C. Lin, J. Mead, R. T. Jaspers, X. Trepat, G. Lenormand, et al. 2009. "Reinforcement versus Fluidization in Cytoskeletal Mechanoresponsiveness." *PloS One* 4 (5). doi:10.1371/journal.pone.0005486.

Kuo, K.-H., A. M. Herrera, and C. Y. Seow. 2003. "Ultrastructure of Airway Smooth Muscle." *Respiratory Physiology & Neurobiology* 137 (2-3).

Lan, B., L. Deng, G. M. Donovan, L. Y. M. Chin, H. T. Syyong, L. Wang, J. Zhang, et al. 2015. "Force Maintenance and Myosin Filament Assembly Regulated by Rho-Kinase in Airway Smooth Muscle." *American Journal of Physiology. Lung Cellular and Molecular Physiology* 308 (1). doi:10.1152/ajplung.00222.2014.

Lan, B., B. A. Norris, J. C.-Y. Liu, P. D. Pare, C. Y. Seow, and L. Deng. 2015. "Development and Maintenance of Force and Stiffness in Airway Smooth Muscle." *Canadian Journal of Physiology and Pharmacology* 93 (3): 163–69. doi:10.1139/cjpp-2014-0404.

Lan, B., L. Wang, J. Zhang, C. D. Pascoe, B. A. Norris, J. C.-Y. Liu, D. Solomon, P. D. Pare, L. Deng, and C. Y. Seow. 2013. "Rho-Kinase Mediated Cytoskeletal Stiffness in Skinned Smooth Muscle." *Journal of Applied Physiology (Bethesda, Md. : 1985)* 115 (10): 1540–52. doi:10.1152/japplphysiol.00654.2013.

Lim, T. K., S. M. Ang, T. H. Rossing, E. P. Ingenito, and R. H. Jr Ingram. 1989. "The Effects of Deep Inhalation on Maximal Expiratory Flow during Intensive Treatment of Spontaneous Asthmatic Episodes." *The American Review of Respiratory Disease* 140 (2): 340–43. doi:10.1164/ajrccm/140.2.340.

Lombardi, V., and G. Piazzesi. 1990. "The Contractile Response during Steady Lengthening of Stimulated Frog Muscle Fibres." *The Journal of Physiology* 431 (December): 141–71.

Martyn, D. A., and A. M. Gordon. 1992. "Force and Stiffness in Glycerinated Rabbit Psoas Fibers. Effects of Calcium and Elevated Phosphate." *The Journal of General Physiology* 99 (5).

Masuo, M., S. Reardon, M. Ikebe, and T. Kitazawa. 1994. "A Novel Mechanism for the Ca(2+)-Sensitizing Effect of Protein Kinase C on Vascular Smooth Muscle: Inhibition of Myosin Light Chain Phosphatase." *The Journal of General Physiology* 104 (2): 265–86.

Mehta, D., and S. J. Gunst. 1999. "Actin Polymerization Stimulated by Contractile Activation Regulates Force Development in Canine Tracheal Smooth Muscle." *The Journal of Physiology* 519 Pt 3 (September): 829–40.

Meiss, R. A. 1987. "Stiffness of Active Smooth Muscle during Forced Elongation." *The American Journal of Physiology* 253 (3 Pt 1): C484–93.

Merkel, L., W. T. Gerthoffer, and T. J. Torphy. 1990. "Dissociation between Myosin Phosphorylation and Shortening Velocity in Canine Trachea." *The American Journal of Physiology* 258 (3 Pt 1): C524–32.

Mijailovich, S. M., J. J. Fredberg, and J. P. Butler. 1996. "On the Theory of Muscle Contraction: Filament Extensibility and the Development of Isometric Force and Stiffness." *Biophysical Journal* 71 (3): 1475–84. doi:10.1016/S0006-3495(96)79348-7.

Miller-Hance, W. C., and K. E. Kamm. 1991. "Force-Velocity Relation and Myosin Light Chain Phosphorylation in Bovine Coronary Arterial Smooth Muscle." *Circulation Research* 69 (5): 1207–14.

Morgan, J. P., and K. G. Morgan. 1984. "Stimulus-Specific Patterns of Intracellular Calcium Levels in Smooth Muscle of Ferret Portal Vein." *The Journal of Physiology* 351 (June): 155–67.

Niiro, N., and M. Ikebe. 2001. "Zipper-Interacting Protein Kinase Induces Ca(2+)-Free Smooth Muscle Contraction via Myosin Light Chain Phosphorylation." *The Journal of Biological Chemistry* 276 (31): 29567–74. doi:10.1074/jbc.M102753200.

Noble, P. B. 2013. "Disruption of the Bronchodilatory Response to Deep Inspiration in Asthma--Extrinsic or Intrinsic to the Airway Smooth Muscle?" *Respiratory Physiology & Neurobiology* 189 (3): 655–57. doi:10.1016/j.resp.2013.10.003.

Noble, P. B., C. D. Pascoe, B. Lan, S. Ito, L. E. M. Kistemaker, A. L. Tatler, T. Pera, B. S. Brook, R. Gosens, and A. R. West. 2014. "Airway Smooth Muscle in Asthma: Linking Contraction and Mechanotransduction to Disease Pathogenesis and Remodelling." *Pulmonary Pharmacology & Therapeutics* 29 (2). doi:10.1016/j.pupt.2014.07.005.

Obara, K., A. Takai, J. C. Ruegg, and P. de Lanerolle. 1989. "Okadaic Acid, a Phosphatase Inhibitor, Produces a Ca2+ and Calmodulin-Independent Contraction of Smooth Muscle." *Pflugers Archiv : European Journal of Physiology* 414 (2): 134–38.

Oliver, M., T. Kovats, S. M. Mijailovich, J. P. Butler, J. J. Fredberg, and G. Lenormand. 2010. "Remodeling of Integrated Contractile Tissues and Its Dependence on Strain-Rate Amplitude." *Physical Review Letters* 105 (15).

Opazo S., Anabelle, W. Zhang, Y. Wu, C. E. Turner, D. D. Tang, and S. J. Gunst. 2004. "Tension Development during Contractile Stimulation of Smooth Muscle Requires Recruitment of Paxillin and Vinculin to the Membrane." *American Journal of Physiology. Cell Physiology* 286 (2): C433–47. doi:10.1152/ajpcell.00030.2003.

Pascoe, C. D., G. M. Donovan, Y. Bosse, C. Y. Seow, and P. D. Pare. 2014. "Bronchoprotective Effect of Simulated Deep Inspirations in Tracheal Smooth Muscle." *Journal of Applied Physiology (Bethesda, Md. : 1985)* 117 (12): 1502–13.

doi:10.1152/japplphysiol.00713.2014.

Pinniger, G. J., K. W. Ranatunga, and G. W. Offer. 2006. "Crossbridge and Non-Crossbridge Contributions to Tension in Lengthening Rat Muscle: Force-Induced Reversal of the Power Stroke." *The Journal of Physiology* 573 (Pt 3): 627–43. doi:10.1113/jphysiol.2005.095448.

Pratusevich, V. R., C. Y. Seow, and L. E. Ford. 1995. "Plasticity in Canine Airway Smooth Muscle." *The Journal of General Physiology* 105 (1).

Puetz, S., L. T. Lubomirov, and G. Pfitzer. 2009. "Regulation of Smooth Muscle Contraction by Small GTPases." *Physiology (Bethesda, Md.)* 24 (December): 342–56. doi:10.1152/physiol.00023.2009.

Pyrgos, G., N. Scichilone, A. Togias, and R. H. Brown. 2011. "Bronchodilation Response to Deep Inspirations in Asthma Is Dependent on Airway Distensibility and Air Trapping." *Journal of Applied Physiology (Bethesda, Md. : 1985)* 110 (2): 472–79. doi:10.1152/japplphysiol.00603.2010.

Qi, D., R. W. Mitchell, T. Burdyga, L. E. Ford, K.-H. Kuo, and C. Y. Seow. 2002. "Myosin Light Chain Phosphorylation Facilitates in Vivo Myosin Filament Reassembly after Mechanical Perturbation." *American Journal of Physiology. Cell Physiology* 282 (6): C1298–1305. doi:10.1152/ajpcell.00554.2001.

Raqeeb, A., Y. Jiao, H. T. Syyong, P. D. Pare, and C. Y. Seow. 2012. "Regulatable Stiffness in Relaxed Airway Smooth Muscle: A Target for Asthma Treatment?" *Journal of Applied Physiology (Bethesda, Md. : 1985)* 112 (3): 337–46. doi:10.1152/japplphysiol.01036.2011.

Roman, H. N., N. B. Zitouni, L. Kachmar, A. Benedetti, A. Sobieszek, and A.M. Lauzon. 2014. "The Role of Caldesmon and Its Phosphorylation by ERK on the Binding Force of Unphosphorylated Myosin to Actin." *Biochimica et Biophysica Acta* 1840 (11): 3218–25. doi:10.1016/j.bbagen.2014.07.024.

Scichilone, N., S. Permutt, V. Bellia, and A. Togias. 2005. "Inhaled Corticosteroids and the Beneficial Effect of Deep Inspiration in Asthma." *American Journal of Respiratory and Critical Care Medicine* 172 (6): 693–99. doi:10.1164/rccm.200407-955OC.

Scichilone, N., T. Kapsali, S. Permutt, and A. Togias. 2000a. "Deep Inspiration-Induced Bronchoprotection Is Stronger than Bronchodilation." *American Journal of Respiratory and Critical Care Medicine* 162 (3 Pt 1): 910–16. doi:10.1164/ajrccm.162.3.9907048.

Scichilone, N., S. Permutt, and A. Togias. 2001a. "The Lack of the Bronchoprotective and Not the Bronchodilatory Ability of Deep Inspiration Is Associated with Airway Hyperresponsiveness." *American Journal of Respiratory and Critical Care Medicine* 163 (2): 413–19. doi:10.1164/ajrccm.163.2.2003119.

Seow, C. Y. 2005. "Myosin Filament Assembly in an Ever-Changing Myofilament Lattice of Smooth Muscle." *American Journal of Physiology. Cell Physiology* 289 (6): C1363–68. doi:10.1152/ajpcell.00329.2005.

Seow, C. Y., and L. E. Ford. 1993. "High Ionic Strength and Low pH Detain Activated Skinned Rabbit Skeletal Muscle Crossbridges in a Low Force State." *The Journal of General Physiology* 101 (4).

Seow, C. Y., V. R. Pratusevich, and L. E. Ford. 2000. "Series-to-Parallel Transition in the Filament Lattice of Airway Smooth Muscle." *Journal of Applied Physiology (Bethesda, Md. : 1985)* 89 (3): 869–76.

Seow, C. Y., and N. L. Stephens. 1987. "Time Dependence of Series Elasticity in Tracheal

Smooth Muscle." *Journal of Applied Physiology (Bethesda, Md. : 1985)* 62 (4): 1556–61.

Siegman, M. J., T. M. Butler, S. U. Mooers, and R. E. Davies. 1976. "Calcium-Dependent Resistance to Stretch and Stress Relaxation in Resting Smooth Muscles." *The American Journal of Physiology* 231 (5 Pt. 1): 1501–8.

Skloot, G., S. Permutt, and A. Togias. 1995a. "Airway Hyperresponsiveness in Asthma: A Problem of Limited Smooth Muscle Relaxation with Inspiration." *The Journal of Clinical Investigation* 96 (5): 2393–2403. doi:10.1172/JCI118296.
1995b. "Airway Hyperresponsiveness in Asthma: A Problem of Limited Smooth Muscle Relaxation with Inspiration." *The Journal of Clinical Investigation* 96 (5): 2393–2403. doi:10.1172/JCI118296.

Sobieszek, A. 1977. "Ca-Linked Phosphorylation of a Light Chain of Vertebrate Smooth-Muscle Myosin." *European Journal of Biochemistry / FEBS* 73 (2): 477–83.

Sobieszek, A., B. Sarg, H. Lindner, and C. Y. Seow. 2010. "Phosphorylation of Caldesmon by Myosin Light Chain Kinase Increases Its Binding Affinity for Phosphorylated Myosin Filaments." *Biological Chemistry* 391 (9): 1091–1104. doi:10.1515/BC.2010.105.

Somlyo, A. P., and A. V. Somlyo. 2003. "Ca2+ Sensitivity of Smooth Muscle and Nonmuscle Myosin II: Modulated by G Proteins, Kinases, and Myosin Phosphatase." *Physiological Reviews* 83 (4): 1325–58. doi:10.1152/physrev.00023.2003.

Somlyo, A. P., and A. V. Somlyo. 2004. "Signal Transduction through the RhoA/Rho-Kinase Pathway in Smooth Muscle." *Journal of Muscle Research and Cell Motility* 25 (8): 613–15. doi:10.1007/s10974-004-3146-1.

Tang, D. D., C. E. Turner, and S. J. Gunst. 2003. "Expression of Non-Phosphorylatable Paxillin Mutants in Canine Tracheal Smooth Muscle Inhibits Tension Development." *The Journal of Physiology* 553 (Pt 1). doi:10.1113/jphysiol.2003.045047.

Tanner, J. A., J. R. Haeberle, and R. A. Meiss. 1988. "Regulation of Glycerinated Smooth Muscle Contraction and Relaxation by Myosin Phosphorylation." *The American Journal of Physiology* 255 (1 Pt 1).

Trepat, X., L. Deng, S. S. An, D. Navajas, D. J. Tschumperlin, W. T. Gerthoffer, J. P. Butler, and J. J. Fredberg. 2007. "Universal Physical Responses to Stretch in the Living Cell." *Nature* 447 (7144): 592–95. doi:10.1038/nature05824.

Tseng, S., R. Kim, T. Kim, K. G. Morgan, and C. M. Hai. 1997. "F-Actin Disruption Attenuates Agonist-Induced [Ca2+], Myosin Phosphorylation, and Force in Smooth Muscle." *The American Journal of Physiology* 272 (6 Pt 1): C1960–67.

Uehata, M., T. Ishizaki, H. Satoh, T. Ono, T. Kawahara, T. Morishita, H. Tamakawa, et al. 1997. "Calcium Sensitization of Smooth Muscle Mediated by a Rho-Associated Protein Kinase in Hypertension." *Nature* 389 (6654): 990–94. doi:10.1038/40187.

Walsh, M. P., and C. Sutherland. 1989. "A Model for Caldesmon in Latch-Bridge Formation in Smooth Muscle." *Advances in Experimental Medicine and Biology* 255: 337–46.

Wang, L., P. D. Pare, and C. Y. Seow. 2000. "Effects of Length Oscillation on the Subsequent Force Development in Swine Tracheal Smooth Muscle." *Journal of Applied Physiology (Bethesda, Md. : 1985)* 88 (6): 2246–50.

Wang, R., Rachel A. C., T. Wang, J. Li, and D. D. Tang. 2014. "The Association of Cortactin with Profilin-1 Is Critical for Smooth Muscle Contraction." *The Journal of Biological Chemistry* 289 (20): 14157–69. doi:10.1074/jbc.M114.548099.

Wang, Z., F. M. Pavalko, and S. J. Gunst. 1996. "Tyrosine Phosphorylation of the Dense Plaque Protein Paxillin Is Regulated during Smooth Muscle Contraction." *The American Journal*

of Physiology 271 (5 Pt 1): C1594–1602.

Warshaw, D. M., and F. S. Fay. 1983. "Cross-Bridge Elasticity in Single Smooth Muscle Cells." *The Journal of General Physiology* 82 (2): 157–99.

Word, R. A., D. C. Tang, and K. E. Kamm. 1994. "Activation Properties of Myosin Light Chain Kinase during Contraction/relaxation Cycles of Tonic and Phasic Smooth Muscles." *The Journal of Biological Chemistry* 269 (34): 21596–602.

Zhang, W., L. Du, and S. J. Gunst. 2010. "The Effects of the Small GTPase RhoA on the Muscarinic Contraction of Airway Smooth Muscle Result from Its Role in Regulating Actin Polymerization." *American Journal of Physiology. Cell Physiology* 299 (2). doi:10.1152/ajpcell.00118.2010.

Zhang, W., and S. J. Gunst. 2006. "Dynamic Association between Alpha-Actinin and Beta-Integrin Regulates Contraction of Canine Tracheal Smooth Muscle." *The Journal of Physiology* 572 (Pt 3): 659–76. doi:10.1113/jphysiol.2006.106518.

Zhang, W., Y. Huang, and S. J. Gunst. 2012. "The Small GTPase RhoA Regulates the Contraction of Smooth Muscle Tissues by Catalyzing the Assembly of Cytoskeletal Signaling Complexes at Membrane Adhesion Sites." *The Journal of Biological Chemistry* 287 (41): 33996–8. doi:10.1074/jbc.M112.369603.

Zhang, W., Y. Wu, L. Du, D. D. Tang, and S. J. Gunst. 2005. "Activation of the Arp2/3 Complex by N-WASp Is Required for Actin Polymerization and Contraction in Smooth Muscle." *American Journal of Physiology. Cell Physiology* 288 (5): C1145–60. doi:10.1152/ajpcell.00387.2004.

Zhao, R., L. Du, Y. Huang, Y. Wu, and S. J. Gunst. 2008. "Actin Depolymerization Factor/cofilin Activation Regulates Actin Polymerization and Tension Development in Canine Tracheal Smooth Muscle." *The Journal of Biological Chemistry* 283 (52): 36522–31. doi:10.1074/jbc.M805294200.